Side Chain Effects in Hybrid PPV/PPE Polymers

Daniel Ayuk Mbi Egbe,*,† Carsten Peter Roll,‡ Eckhard Birckner,§ Ulrich-Walter Grummt,§ Regina Stockmann,† and Elisabeth Klemm*,†

Institut für Organische Chemie und Makromolekulare Chemie der Friedrich-Schiller-Universität Jena, Humboldtstrasse 10, D-07743 Jena, Germany; Institut für Anorganische und Analytische Chemie der Friedrich-Schiller-Universität, August-Bebel-Strasse 2, D-07743 Jena, Germany; and Institut für Physikalische Chemie der Friedrich-Schiller-Universität Jena, Lessingstrasse 10, D-07743 Jena, Germany

Received December 18, 2001; Revised Manuscript Received February 19, 2002

ABSTRACT: The Horner−Wadsworth−Emmons olefination reaction of luminophoric dialdehydes **1** and **2** and bisphosphonates **3** provide high-molecular-weight and thermostable PPV/PPE hybrid polymers **4** and **5** of well-defined general constitutional structure −(CH═CH−Ph−CH═CH−Ph−C≡C−Ph−C≡C−Ph−)$_n$, which was confirmed by NMR, infrared and elemental analysis. Soluble and good film-forming materials were obtained after attaching long linear alkoxy, e.g., dodecyloxy, octadecyloxy, or branched alkoxy side chains, e.g., 2-ethylhexyloxy, on the conjugated backbone. Thermotropic and lyotropic liquid crystalline behavior was observed with polarized optical microscopy. The presence of triple bonds along the PPV backbone increases the electron affinity of these polymers, which is reflected by the comparatively (with MEH−PPV) higher oxidation potential of 1.30 V vs Ag/AgCl. Polymers **4** and **5** are good photoconducting and highly luminescent materials. While almost identical photophysical behaviors for all polymers of type **4** ($\lambda_{max,abs}$ = 450 nm, $\lambda_{max,em}$ = 490 nm) or **5** ($\lambda_{max,abs}$ = 470 nm, $\lambda_{max,em}$ = 553 nm) were obtained in dilute chloroform solution, resulting in fluorescence quantum yields between 70 and 80% of the yellowish-green emission, the solid-state properties (color, thermal behavior, photoconductivity, absorption and emission spectra, and photoluminescence quantum yields) are dependent on the *size*, *geometry*, *number*, and *location* of the grafted alkoxy side groups. Exchanging for example the position of the side chains from **4ac** ($R^2 = O(CH_2)_{17}CH_3$, $R^4 = O(CH_2)_7CH_3$) to **4ca** ($R^2 = O(CH_2)_7CH_3$, $R^4 = O(CH_2)_{17}CH_3$) leads not only to a change in color of the material from orange to yellow but also a dramatic change in the photophysical behavior. In general, octadecyloxy side chains in position R^4 are necessary to obtain narrow and structured emission curves, small Stokes shifts, less excimer formation, and higher fluorescence quantum yields (30−40%). The fully substituted, deep orange-red polymer **5a** ($R^2 = R^4 = O(CH_2)_{17}CH_3$), for example, behaves as if its conjugated backbone was *dissolved* in a hydrocarbon solvent. This is confirmed by its very high photocurrent of 1.1×10^{-9} A (which is at least 2 orders of magnitude higher than that of all the other polymers), detected at the lowest threshold voltage of 10 V, and its highest ϕ_{fl} value of 54%. It can be assumed from these facts that photoconductivity is more an intramolecular phenomenon than an intermolecular one. Strong $\pi-\pi$ interchain interactions not only lead to fluorescence quenching through excimer formation but also have a negative effect on photoconductivity.

Introduction

Conjugated polymers have attracted considerable attention in the last two decades due to their potential use in a wide range of applications in electronics and photonics, favored by their ease of preparation, their tunable electronic and optical properties, and their ease of processability.[1−4] Derivatives of poly(*p*-phenylenevinylene) (PPV) have been intensively studied since electroluminescence was reported in this class of polymers by the group of Holmes.[5] Most PPV derivatives have low electron affinity which is reflected by the low electroluminescence efficiencies obtained from their monolayered light-emitting diodes (LEDs).[4,5] High electron affinity is a prerequisite for the fabrication of LEDs with good electron injection from metal electrodes other than calcium, thus avoiding the need to encapsulate the cathode.[6]

One approach to achieve high electron affinity is to attach electron-withdrawing groups either on the vinylene position, like in cyano-substituted PPVs,[6−9] or onto the aromatic ring, like in halogen- (Cl-, Br-) substituted PPVs[10] and in trifluoromethyl-substituted PPVs.[11] Another approach is to use electron-deficient rings in the polymer backbone, like in the case of poly(*p*-pyridylene vinylene)s.[12,13] A further alternative and most recent approach to obtain an approximately balanced hole-injection and electron uptake, which has been designed independently by the group of Bunz[14] and our group,[15] is to incorporate the electron-withdrawing acetylene group in the PPV backbone, leading to hybrid PPV/PPE polymers. We synthesized polymers **4** with a well-defined general structure, −(CH═CH−Ph−CH═CH−Ph−C≡C−Ph−C≡C−Ph−)$_n$, having two alkoxy side chains (octyloxy, dodecyloxy, and octadecyloxy) in every second phenyl ring.[15] Horner−Wadsworth−Emmons[16] polycondensation reaction of dialdehydes with bisphosphonate esters was the chosen synthetic route, because of the efficiency of this method and the resulting double bonds have an all-trans (*E*) configuration. Moreover, defect-free polymers are obtained.

Alkoxy chains, grafted as side groups on the backbone of conjugated polymers, do not only enhance their

* Corresponding author. E-mail: c5ayda@uni-jena.de or c9klel@rz.uni-jena.de.
† Institut für Organische Chemie und Makromolekulare Chemie der Friedrich-Schiller-Universität Jena.
‡ Institut für Anorganische und Analytische Chemie der Friedrich-Schiller-Universität Jena.
§ Institut für Physikalische Chemie der Friedrich-Schiller-Universität Jena.

10.1021/ma012195g CCC: $22.00
Published on Web 04/06/2002

Scheme 1

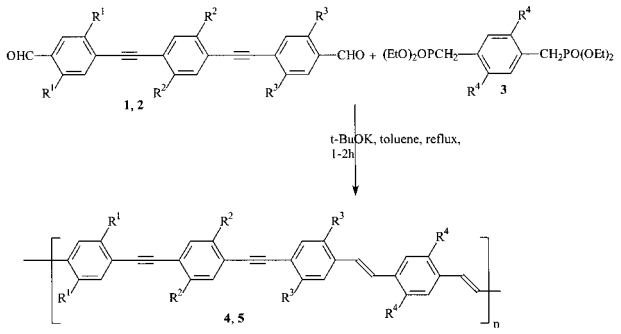

1 : $R^1 = R^3$ = H, **1a** : R^2 = octadecyloxy; **1b** : R^2 = dodecyloxy; **1c** : R^2 = octyloxy; **1d** : R^2 = (2-ethyl)hexyloxy.

2 : $R^1 = R^3$ = octyloxy, R^2 = octadecyloxy.

3a : R^4 = octadecyloxy; **3b** : R^4 = dodecyloxy; **3c** : R^4 = octyloxy; **3d** : R^4 = (2-ethyl)hexyloxy.

4: $R^1 = R^3$ = H, **4aa** : $R^2 = R^4$ = octadecyloxy; **4bb** : $R^2 = R^4$ = dodecyloxy; **4cc** : $R^2 = R^4$ = octyloxy; **4dd** : $R^2 = R^4$ = (2-ethyl)hexyloxy; **4ab**: R^2 = octadecyloxy, R^4 = dodecyloxy ; **4ac** : R^2 = octadecyloxy, R^4 = octyloxy; **4ad**: R^2 = octadecyloxy, R^4 = (2-ethyl)hexyloxy; **4ba** : R^2 = dodecyloxy, R^4 = octadecyloxy; **4ca** : R^2 = octyloxy, R^4 = octadecyloxy; **4da** : R^2 = (2-ethyl)hexyloxy, R^4 = octadecyloxy.

5 : $R^1 = R^3$ = octyloxy, **5a** : $R^2 = R^4$ = octadecyloxy; **5c** : $R^2 = R^4$ = octyloxy

solubility and subsequently their processability into thin films for various applications, but can also lead to dramatic changes in optical, electronic and transport properties as well as thermal behavior that conjugated polymers show in the solid state.[17] Preliminary investigations on polymers **4aa**, **4bb**, **4cc**, **4ab**, and **4ac** confirm this assertion.[15] However, to have a better understanding of the influence of alkoxy side chains on the properties of this new type of polymers, it was necessary to synthesize further polymers of type **4** (having two substituents in every second phenyl ring) and polymers of type **5** (having two substituents in every phenyl ring), taking into consideration the *geometry* (linear or branched), the *size*, the *position* (attached on phenyl rings adjacent to the double or triple bonds), and the *number* of the side groups (Scheme 1). In this article we report the synthesis of polymers **4dd**, **4ba**, **4ca**, **4ad**, **4da**, **5a**, and **5c**; we compare their thermal behavior in the solid state, photoconductivity, and photophysical behavior in solution as well as in solid state with those of the polymers mentioned above.[15]

Results and Discussion

To obtain high-molecular-weight polymers **4** and **5** under step-growth polymerization conditions,[18] it is necessary to introduce an equivalent of dialdehydes **1**, **2** and bisphosphonate esters **3** into the reaction medium.

The synthesis of dialdehydes **1a**−**c** and the bisphosphonate esters **3a**−**c** have been described elsewhere.[15] The synthetic pathways to dialdehyde **1d** and bisphosphonate **3d** are illustrated in Scheme 2. The synthesis of **3d** started with the bromomethylation of 1,4-di(2-ethyl)hexyloxybenzene **6**[19] using $NaBr/H_2SO_4$ and paraformaldehyde in acetic acid. The bis(bromomethyl) derivative **11** (88%) was finally converted to **3d** by the Michealis−Arbuzov reaction[20] in 99.9% yield. **3d** is a colorless oil which solidifies when kept under 18 °C. The dialdehyde **1d** was synthesized from the Pd-catalyzed Heck−Cassar−Sonogashira−Hagihara[14a,21] cross coupling reaction of diethynyl derivative **9** (obtained in 89% yield from a three steps reaction from **6** over the diiodo

Scheme 2[a]

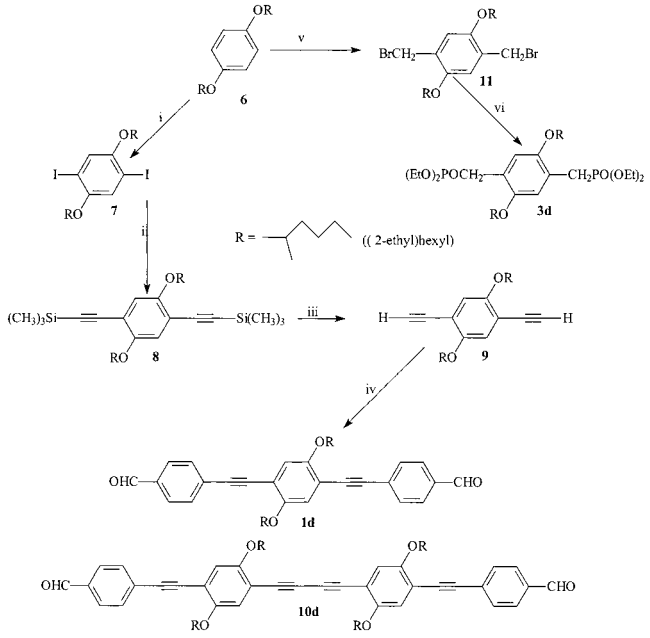

[a] Key: (i) I_2, KIO_3, H_2SO_4, CH_3COOH; (ii) $(CH_3)_3SiC_2H$, $Pd(PPh_3)_2Cl_2/CuI$, iPr_2NH; (iii) KOH/MeOH, THF; (iv) 4-bromobenzaldehyde, $Pd(PPh_3)_4/CuI$, iPr_2NH, toluene, Ar; (v) $(CH_2O)_n$, $NaBr/H_2SO_4$, CH_3COOH; (vi) $P(OEt)_3$.

derivative **7**[19] and the bis(trimethylsilyl)acetylene derivative **8** (77%)) with 2 equiv of 4-bromobenzaldehyde. Compound **1d** was obtained in 67% yield as a bright yellow substance alongside the oxidative coupling product **10d** (0.78%). Both substances were separated through chromatography on a silica gel column using toluene as eluent. The yield of **10d** is lower than those of **10a** (R = octadecyl, 2.20%) **10b** (R = dodecyl, 3.1%) and **10c** (R = octyl, 1.50%)[15] because the reaction was carried out while flushing the reaction mixture with argon to keep oxygen away as much as possible, thus suppressing the Cu-catalyzed oxidative coupling reaction of acetylenes to diacetylenes. Figure 1 depicts the ^{13}C NMR (62 MHz, $CDCl_3$) spectra of **1d** and **10d**. These spectra are similar to those of **1a**−**c** and **10a**−**c** respectively,[15] except for the new peaks appearing at 11 and 40 ppm assigned for carbons C_h and C_b, respectively, as a result of the branching in the 2-ethylhexyloxy side group. Scheme 3 illustrates the synthetic pathway used to obtain the dialdehyde **2**, a prerequisite for the synthesis of polymers of type **5**. The Bouveault formylation[22] of 1,4-dibromo-2,5-dioctyloxybenzene (**12**)[23] using 1 equiv each of butyllithium and dimethylformamide in diethyl ether and keeping the temperature between 10 and 15 °C led to 1-formyl-4-bromo-2,5-dioctyloxybenzene (**13**) in 61% yield. Solubility problems in diethyl ether at low temperatures did not allow the synthesis of monoformyl-derivatives with longer side chains (e.g., dodecyl, octadecyl). The subsequent Pd-catalyzed cross coupling reaction of 1,4-diethynyl-2,5-dioctadecyloxybenzene (**14**)[23] with 2 equiv of **13** gave **2** in 60% yield as a light bright yellow substance. As expected, **2** was obtained alongside the diacetylene derivative **15** (3%). Both compounds were also separated through chromatography on a silica gel column using toluene as eluent and were characterized. Figure 2 presents the ^{13}C NMR (100 MHz, $CDCl_3$) spectrum of **2** and the ^1H NMR (250 MHz, $CDCl_3$) spectrum of **15**. The carbons of the alkyl side chains are dominating upfield in the region of 14

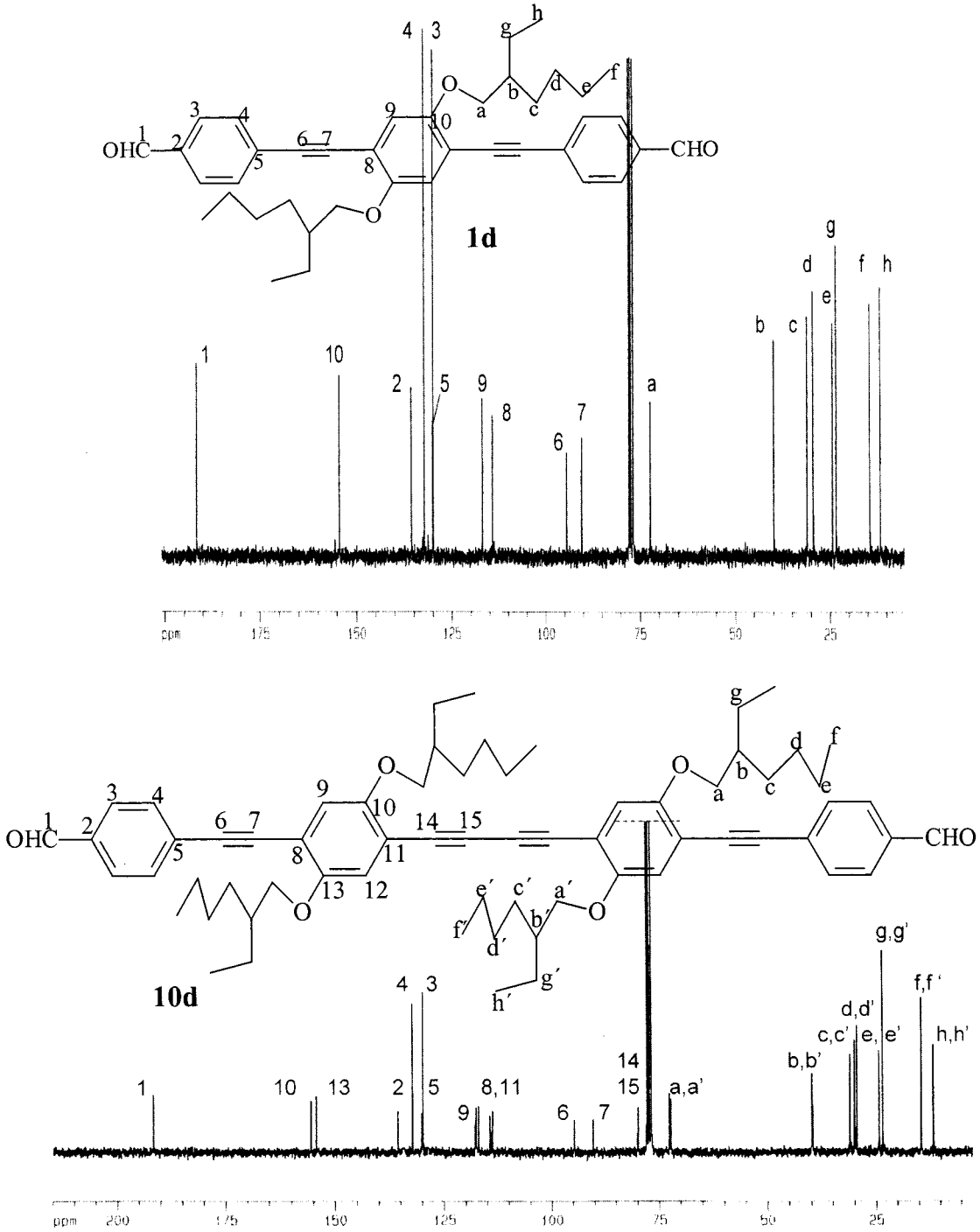

Figure 1. ^{1}H NMR (62 MHz, $CDCl_3$) spectra of monomers **1d** and **10d**.

to 32 ppm. The three different methylene carbons adjacent to oxygen are found around 69 ppm. The acetylenic carbons signals are located at 91 and 94 ppm. The peaks downfield between 110 and 156 ppm are assigned to the aromatic carbons. The aldehyde carbon is detected at 189 ppm. Both ^{13}C and ^{1}H NMR spectra of **2** prove that **2** is a symmetric molecule. The NMR data of **15**, on the contrary, reveal a non symmetric molecule. This can be attributed to a strong nonplanar conformation around the diyne unit as a result of the steric hindrances among the long alkoxy side chains. The presence of a diyne unit in **15** is confirmed by the aromatic proton resonance around 6.9 ppm. The locations of the rest of protons signals of **15** are similar to those of **2**. The dissymmetry in **15** gives rise to a multitude of peaks in ^{13}C NMR in the regions as described above for **2**.

The polymers were synthesized using the Horner−Wadsworth−Emmons (HWE) olefination reaction of dialdehydes **1** and **2** with bisphosphonates **3** in the different combinations shown in Scheme 1. Toluene was used as solvent and an excess of potassium *tert*-butoxide as base. Short reaction times (1.5−2 h) were necessary due to the high efficiency of the HWE reaction. Polymers **4dd, 4ba, 4ac, 4ad, 4da**, **5a** and **5c** were obtained in yields of up to 88% after workup. Number-average molecular weights $\bar{M}_n$, obtained through GPC in THF and based on polystyrene standards, were between 30 000 and 80 0000, with polydispersity indices lying between 2 and 4.5, which are consistent with HWE

Scheme 3

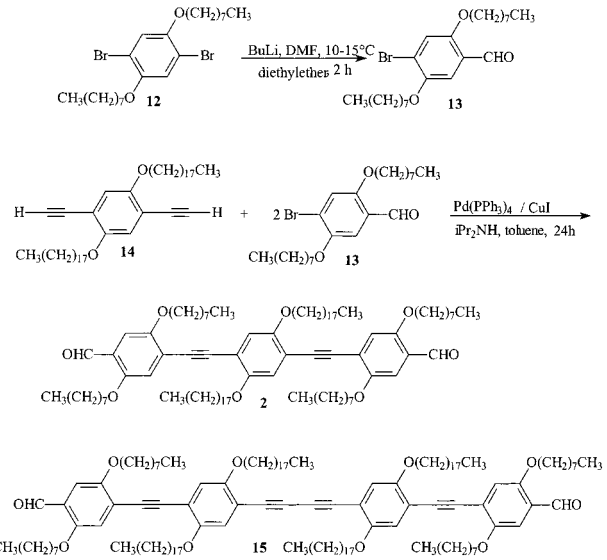

reaction conditions. $\bar{M}_n$ values of 23600 and 27000 for **5a** and **5c,** respectively, obtained through VPO in $CHCl_3$, are approximately the same as those from GPC (Table 1). The polymers are soluble in organic solvents such as THF, toluene, $CHCl_3$, CH_2Cl_2, chlorobenzene, etc, but poor solubility was noticed in 1,4-dioxane; they can be processed into transparent films. Contrary to polymer **4cc** ($R^2 = R^4 =$ octyloxy),[15] which showed virtually no solubility, polymer **4dd** ($R^2 = R^4 =$ 2-ethylhexyloxy) having the branched isomer as substitutents, showed very good solubility. It has a yellow color instead of the orange color found in **4cc**. Exchanging the positions of the side chains, like in **4ac** and **4ca**, leads to changes in color of the materials from bright orange to yellow. In general, all the polymers of type **4** with branched side chains (**4dd**, **4ad**, **4da**) and linear side chains R^4 equal to or longer than dodecyloxy are yellow and those with side chains R^4 equal to octyloxy are orange materials. This is an indication of the influence of side chains in the aggregation modes in solid state. Polymer **5c** has a carrotlike orange-red color, while **5a** is a deep orange-red material.

The polymers were characterized through ^1H and ^{13}C NMR, IR (KBr pellets) spectroscopy and elemental analysis. The NMR spectra of the new polymers of type **4** are similar to those already published,[15] except that the polymers **4dd**, **4ad**, and **4da**, having 2-ethylhexyloxy as side chains, are moreover characterized with carbon peaks at 11 and 40 ppm. Figure 3 shows the ^{13}C NMR (100 MHz, $CDCl_3$) of polymer **5c**. As expected, the carbons of the alkyl side side chains are found between 14 and 32 ppm. The relatively broad signal around 70 ppm, composed of signals at 69.43, 69.83, and 70.02 ppm, can be attributed to the three environmentally different carbons adjacent to the oxygen atom. The triple bonds carbons are located at 91 and 92 ppm. The downfield signals between 110 and 154 ppm derived from the aromatic and the vinylene carbons. In the ^1H NMR (400 MHz, $CDCl_3$) the vinylene H peak at 7.46 ppm having a coupling constant $^3J = 16.90$ Hz is an indication of the all-trans (*E*) configuration of the double bonds. The lack of aldehyde function signals in ^1H and ^{13}C NMR is consistent with the high molecular weights obtained for these compounds.

The new compounds are thermostable. The start of the thermal degradation under air for the polymers of type **4** lies between 300 and 350 °C, where 5% weight loss was recorded (Table 2). The polymer of type **5** exhibit comparatively higher thermal stability. Their thermal decomposition under air starts above 360 °C. The DSC measurements carried at a heating rate of 10 K/min and a cooling rate of −10 K/min show a continuous and reversible phase transition behavior for the novel polymers, except for polymer **4cc**, having octyloxy as side chains, and all the polymers with 2-ethylhexyloxy as side goups, **4dd**, **4ad**, and **4da**. For polymers of type **4**, reversible transitions were obtained when the heating was kept under 200 °C. Heating up to 300 °C was possible for polymers of type **5.** The transition temperatures are listed in Table 2. Figure 4 illustrates the heating and cooling curves of polymers **4ac**, **4ca**, **5a**, and **5c**. Exchanging the position of the side chains, like in **4ac** and **4ca** as well as in **4ab** and **4ba**, brings about very little change in the heating and cooling curves. While the heating of **4ac** leads to an endothermic peak at 135 °C, that of **4ca** gives the same transition at 132 °C. The cooling traces depict broad exothermic peaks at 110 and 100 °C, respectively. Likewise the heating curves of **4ab** and **4ba** are characterized with closely located sharp endothermic peaks at 100 and 105 °C respectively; their exothermic transitions at 65 and 63 °C from the cooling curves are almost the same. The heating of polymers of type **5** leads to comparatively higher endothermic transitions, e.g., 213 °C for **5a** and 217 °C for **5c**. While the cooling curve of **5a** is characterized with one broad exothermic peak at 55 °C and one very sharp exothermic at 178 °C, the cooling trace of **5c** consists of two broad closely located exothermic peaks at 147 and 171 °C. These transitions could not be exactly assigned to glass transitions nor to glass-to-liquid-crystal transitions.

However polarized optical microscopy (POM) indicates thermotropic mesomorphic behavior. Heating and cooling rates for thermotropic measurements were 10 K/min. On heating, the compounds show transitions from the glassy state to a homeotropic liquid crystal phase of lower viscosity. The compounds display birefrigence on shearing.

For compounds with linear alkyloxy side chains of type **4**, this transition occurs at temperatures between 170 and 250 °C. The polymers of type **5** melt into a nematic phase around 210 °C which correlates with the endothermic transitions at 213 for **5a** and 217 °C for **5c** found in DSC measurements.[24] Although growth of characteristic mesophase texture was not achieved, the fluidity indicates the presence of a thermotropic nematic phase. This is well-known from other main chain liquid-crystalline polymers with rigid-core architecture and lateral alkyl or alkyloxy substitution.[25] The introduction of branched alkyloxy chains in polymers **4dd**, **4ad**, and **4da** leads to an increase in viscosity rendering mesophase characterization nearly impossible. Yet at temperatures above 130 °C, birefringence was observed.

All compounds have been observed to form lyotropic mesophases in nonpolar solvents such as dichloromethane or chloroform. Lyotropic measurements were carried out at room temperature. **4ca** displays in dichloromethane a nematic Schlieren-type texture as depicted in Figure 5.

The new compounds can be oxidized and reduced by differential pulse polarography (DPP). Cyclic voltammetry investigations were void of clear oxidation peaks; in constrast clear and reversible reduction potential

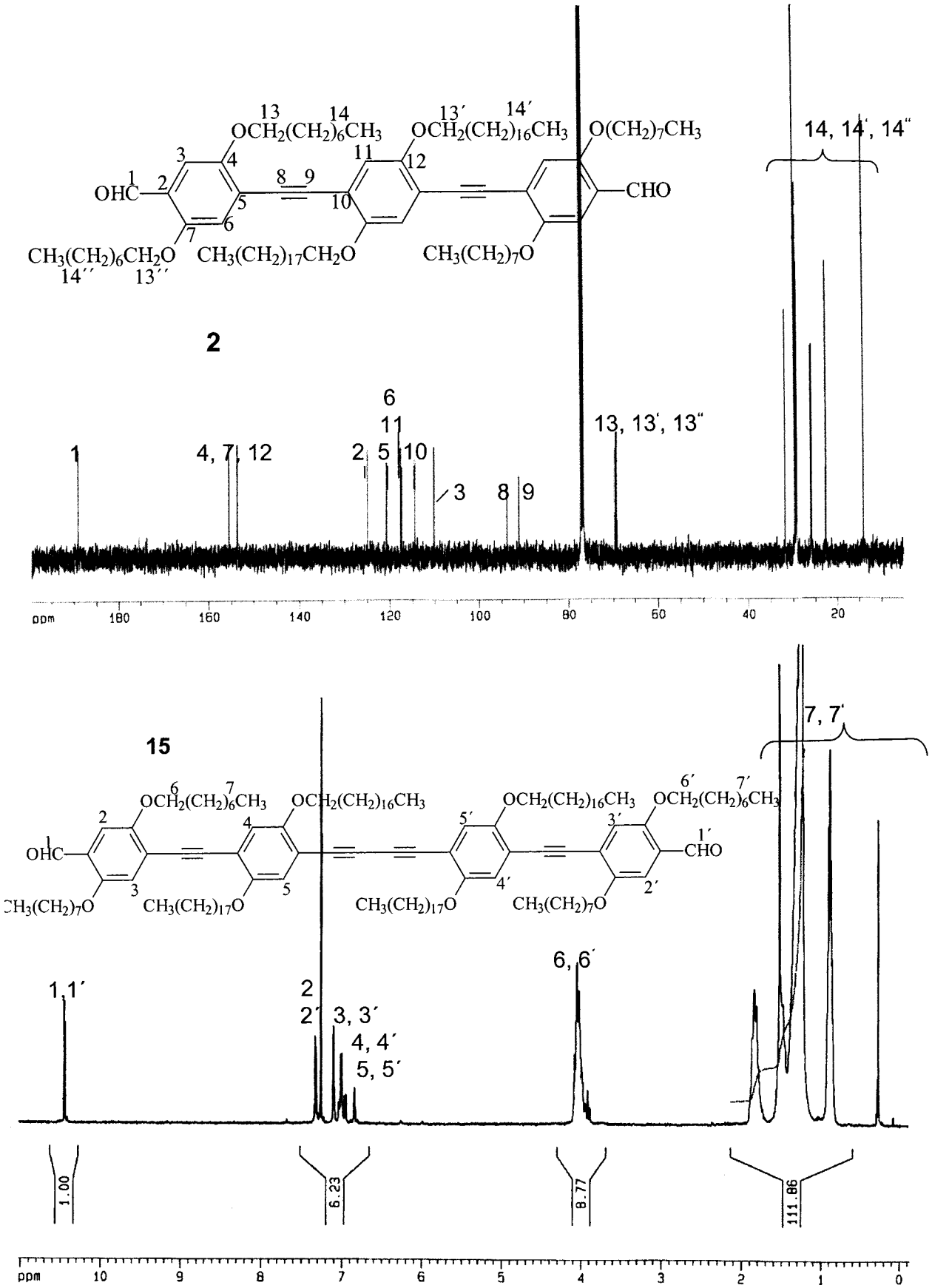

Figure 2. ^{13}C NMR (100 MHz, $CDCl_3$) spectrum of monomer **2** and ^{1}H NMR (250 MHz, $CDCl_3$) of monomer **15**.

curves were obtained by this method.[15] The polymers are characterized with an oxidation potential of 1.30 V vs Ag/AgCl and a reduction potential of −1.10 V vs Ag/AgCl (Table 3), which are relatively higher than the redox potentials of MEH−PPV (E^{ox} = 0.70 V vs Ag/AgCl, E^{red} = −1.72 V vs Ag/AgCl).[26] This is due to the electron-

Table 1. Data from GPC (THF)

compound	$\bar{M}_n$	$\bar{M}_w$	$\bar{M}_z$	M_p	$\bar{M}_w/\bar{M}_n$	$\overline{DP}$
4aa[a]	37 200	165 900	680 800	126 800	4.4	25
4bb[a]	88 100	551 900	1240 000	1245 000	6.2	77
4ab[a]	74 320	452 900	991 500	1015 000	6.0	56
4ac[b]	57 910	351 600	1154 000	182 300	6.0	48
4dd[a]	35 240	161 700	528 200	89 360	4.5	38
4ba[a]	39 200	166 600	544 300	94 260	4.2	30
4ca[a]	50 000	156 900	425 000	97 000	3.1	42
4ad[a]	60 400	253 200	663 200	143 900	4.1	50
4da[a]	42 320	130 100	329 800	93 770	3.0	35
5a[c]	27 440	62 370	147 800	53 250	2.2	14
	23 600[d]					12[d]
5c[c]	29 410	82 470	200 300	66 530	2.8	17
	27 000[d]					16[d]

[a] Yellow material. [b] Orange material. [c] Orange-red material. [d] Obtained from vapor pressure osmometry in $CHCl_3$.

withdrawing nature of −C≡C−.[27] An average electrochemical band gap energy of 2.40 eV is obtained from these values.

Photoconductivity was observed for all polymers **4** and **5**. The *size*, *geometry*, *position*, and *number* of the side groups have an influence on the photoconducting properties. Among polymers of type **4**, those with linear side chains equal or longer than dodecyloxy, like in the case of **4aa**, **4bb**, and **4ab**,[15] or with branched side chains, like in the case of **4dd**, require a lower threshold voltage (20 V) to detect photoconductivity than those with octyloxy side chains, like in **4ac** and **4ca** (200 V or 400 V). Exchanging the positions of the side chains from **4ac** to **4ca** leads to an increase of the photocurrent (I_{Ph}). (Figure 6A and Table 3).

Polymers of type **5**, with side chains on every phenyl ring, are readily photoconductive at a threshold voltage of 10 V. Polymer **5a** ($R^2 = R^4 = OC_{18}H_{37}$) shows the highest photoconductivity among all the new compounds. Its maximal photocurrent found at 1.1×10^{-9} A at 20 000 cm^{-1} is 2 orders of magnitude higher than that of **5c**, found at 3.9×10^{-11} A at 18 900 cm^{-1} (Figure 6B, Table 3). From these results, one can assume that photoconductivity is basically an intramolecular phenomenon. The conjugated backbone of **5a** behaves as if it was *dissolved* in a hydrocarbon solvent in the solid state.[28] The side groups hinder, to a great extent, strong $\pi-\pi$ interchain interactions, which seem to have a negative effect on photoconductivity.

The photophysical characteristics of the new compounds were investigated by UV−vis absorption and photoluminescence in dilute $CHCl_3$ solution as well as in solid state. Results from the absorption and emission spectra are summarized in Tables 4 and 5. All emission data given here were obtained after exciting at the wavelength of the main absorption band. There is similarity between the absorption and excitation spectra.

Figure 7 shows the absorption and emission spectra of monomers **1d** and its diyne derivative **10d** as well as **2** and its diyne partner **15**. The absorption maximum of **10d**, at $\lambda_{max,abs} = 421$ nm ($\epsilon = 64\,500$) is 23 nm redshifted relative to that of **1d**, at $\lambda_{max,abs} = 398$ nm ($\epsilon = 41\,700$), due to the comparatively longer conjugation segment of **10d**. This bathochromic shift is a general observation when comparing all monomers of type **10** with those of type **1**.[15] Among the monomers of type **10** **10d**, with branched side chains, shows a ca. 10 nm redshift relative to **10a**−**c**, with linear side groups. While the emission curve of **1d**, showing its maximum at $\lambda_{max,em} = 463$ nm, is structureless, **10d** is characterized with a relatively structured and narrow emission spectrum, having its maximum at $\lambda_{max,em} = 468$ nm and a shoulder around 500 nm. Identical emission maxima in chloroform at around $\lambda_{max,em} = 463$ nm were obtained for **1a**−**c** and **10a**−**c**. The fluorescence quantum yields were found to be around 80 and 70% for **1** and **10** respectively.

The strongly nonplanar conformation of **15** at the ground state, as revealed by ^1H and ^{13}C NMR spectroscopies, due the steric hindrance of the side groups and the low rotational barrier around the −C≡C−C≡C− and −C≡C− moieties, leads to a 13 nm blue shift of its absorption maximum, found at a $\lambda_{max,abs} = 409$ nm ($\epsilon = 60\,300$), relative to its dyne-free counterpart **2**, whose absorption maximum was found at $\lambda_{max,abs} = 422$ nm ($\epsilon = 60\,750$). The emission maximum of **15** at $\lambda_{max,em} = 470$ nm, on the contrary, is 4 nm slightly red shifted to that of **2** at $\lambda_{max,em} = 466$ nm, due to a more planar geometry of the conjugated backbone in the first excited state.[29] The fluorescence quantum yields of **2** and **15** amounted to 73 and 59% respectively.

Irrespective of the size and the geometry of the side groups, all polymers of type **4** exhibit similar photophysical behavior in solution. The peak of their absorption curves lies around $\lambda_{max,abs} = 450$ nm, and the emission spectra are characterized by a maximum at $\lambda_{max,em} = 490$ nm and a shoulder around 520 nm. Absorption coefficients between 80 000 and 110 000 and an average optical band gap energy of 2.50 eV were obtained. High fluorescence quantum yields between 70 and 80% of the yellowish-green emission were obtained. Figure 8 presents the absorption and emission spectra of **4dd** and of **5c** in dilute chloroform solution, as representatives of polymers of type **4** and **5** respectively. The higher number of alkoxy side chains in **5** lead to a bathochromic shift of their absorption and emission spectra relative to those of **4**. The absorption maximum of **5a** in chloroform at $\lambda_{max,abs} = 468$ nm ($\epsilon = 86\,300$) is 4 nm blue shifted to that of **5c** at $\lambda_{max,abs} = 472$ nm ($\epsilon = 101\,160$). An optical band gap energy of 2.30 eV was obtained for these compounds. The identical emission curve for both **5a** and **5c**, which is similar in shape to that of **4**, consists of a maximum at $\lambda_{max,em} = 519$ nm and a shoulder at 560 nm. Also high fluorescence quantum yields of around 70% were obtained for this class of compounds.

While the photophysical properties of polymers **4** and **5** in solution are essentially independent of the grafted alkoxy side groups, the solid-state properties were found to be dependent on the *size*, *geometry*, *position*, and *number* of the side chains. Polymers of type **4** can be divided into two groups, namely those with only linear side groups (Figure 9) and those with branched side chains (Figure 10).

Polymer **4ac** ($R^2 = O(CH_2)_{17}CH_3$; $R^4 = O(CH_2)_7CH_3$) has a solid-state absorption band centered at $\lambda_{max,abs} = 465$ nm, its emission maximum is located at $\lambda_{max,em} = 602$ nm, leading to a large Stokes shift of 137 nm and a lower fluorescence quantum yield of 19%. The emission trace of **4ac** consists additionally of two shorter wavelength shoulders at 512 and 556 nm. The relatively short octyloxy side chains at position R^4 (adjacent to the vinylene units), in combination with the fact that every second phenyl unit is unsubstituted, enable strong $\pi-\pi$ interchain interaction, leading to the formation of excimers which provide radiationless decay channels for the excited states and hence resulting in very large

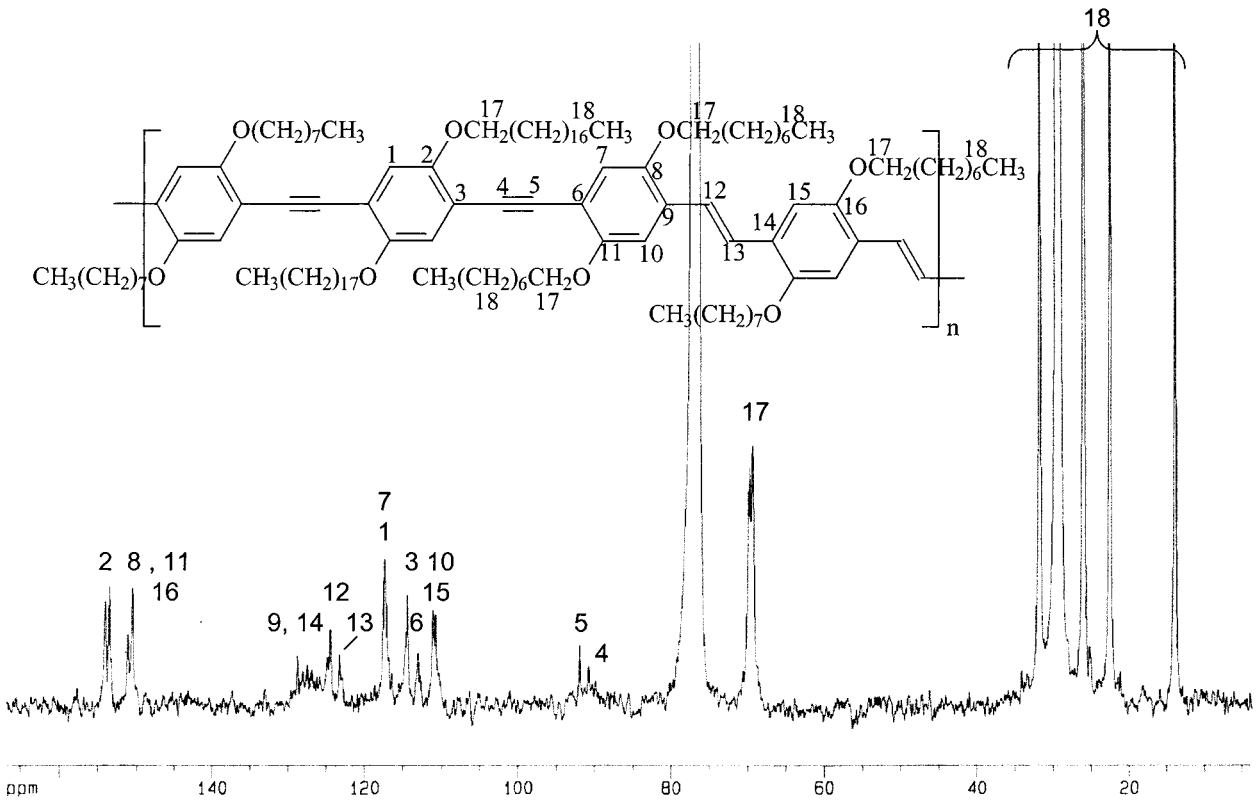

Figure 3. ^{13}C NMR (100 MHz, $CDCl_3$) spectrum of polymer **5c**.

Table 2. Thermal Stabilities and DSC Measurements of the Polymers

compound	$T_{5\%}$/°C[a]	$T_{10\%}$/°C[a]	T_{endo}/°C[b]	T_{exo}/°C[b]
4aa	350	424	95, 136	80
4bb	335	369	70, 167	62, 110
4dd	329	339		
4ab	303	315	100	65
4ba	339	364	105	63
4ac	321	336	55, 135	45, 110
4ca	327	339	132	100
4ad	333	350	60 (irrev)	
4da	313	327	66 (irrev)	
5a	361	400	75, 213	55, 178
5c	386	424	47, 217	147, 171

[a] Thermogravimetric analysis: heating rate 10 K/min under air; values given for weight loss of 5% and 10%. [b] DSC measurements: heating rate at 10 K/min and cooling rate at −10 K/min.

Stokes shift and lower fluorescence quantum yields.[28−30] In the case of **4ca** ($R^2 = O(CH_2)_7CH_3$; $R^4 = O(CH_2)_{17}CH_3$), where the position of the side groups have been exchanged relative to **4ac**, as in the cases of **4aa**, **4bb**, **4ab**,[15] and **4ba**, where the side chains R^2 and R^4 are equal to or longer than $O(CH_2)_{11}CH_3$, almost similar solid-state properties were observed. The absorption spectra consist of a peak with double maxima: a shorter wavelength maximum at ca. 455 nm and a longer one at ca. 480 nm. The structured emission spectra of these polymers have an intense peak at around $\lambda_{max,em} = 510$ nm and a less intense peak around $\lambda_{max,em} = 540$ nm, showing a Stokes shift of ca. 30 nm, which is comparatively smaller than that of **4ac**. The large blue shift of around 94 nm of the emission maximum of these polymers proves that the longer side chains at position R^4 can indeed significantly hinder the interchain interactions, which correlate with the improved fluorescence quantum yields of around 30−40% of these compounds. There is approximately an overlap of the two emission

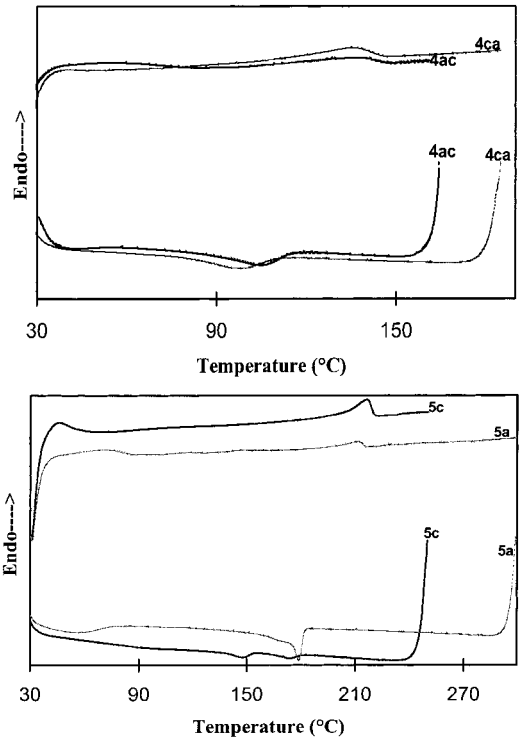

Figure 4. Differential scanning calorimetry heating and cooling traces of polymers **4ac**, **4ca**, **5a**, and **5c** obtained at a heating rate of 10 °C/min and a cooling rate of −10 °C/min.

bands of these polymers with the two shoulder emission bands of **4ac**, proving that the emission spectrum of **4ca** is a superimposition of emissions from fluorophores of isolated excited polymers chains (512 and 556 nm) and from excimers (602 nm). The large Stokes shift of 125 nm obtained in the case of **4cc** ($\lambda_{max,\ abs} = 459$ and 482

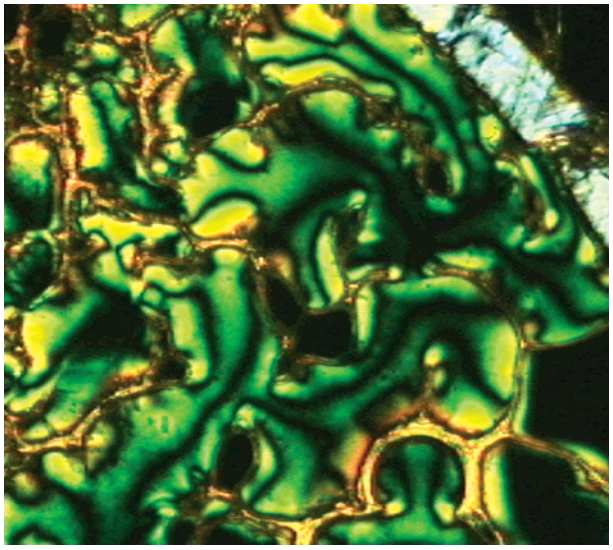

Figure 5. Nematic Schlieren-type texture of **4ca** as revealed by the polarized optical microscopy.

Table 3. Redox Potentials (E^{ox}, E^{red}) and Electrochemical Band Gap Energy (E_g^{ec}) from Differential Pulse Polarography; Photo Currents(I_{ph}) from Photoconductivity Spectra (Surface Cell, Slit Width, 0.2 mm; Light Intensity, 20 μW; Voltage, 10,[a] 20,[b] and 400 V[c]

compound	E^{ox} (vs Ag/AgCl)/V	E^{red} (vs Ag/AgCl)/V	$E_g$ec/eV	I_{ph}/A (ν_{max}/cm^{-1})
4ba	1.40	−1.10	2.50	6.8×10^{-11} (20 400)[c]
4ac	1.34	−1.02	2.36	8.4×10^{-11} (20 000)[c]
4ca	1.39	−1.09	2.48	2.4×10^{-10} (20 200)[c]
4dd	1.42	−1.10	2.52	4.4×10^{-11} (20 000)[b]
4ad	1.39	−1.08	2.47	
4da	1.34	−1.10	2.44	
5a	1.20	−1.10	2.30	1.1×10^{-9} (20 000)[a]
5c	1.41	−1.07	2.48	3.9×10^{-11} (18 900)[a]

nm, $\lambda_{max,em}$ = 584 nm) and its broad and diffuse emission curve once more confirm the assertion that shorter linear side chains (octyloxy at R^4) enable strong excimers formation; however, no fluorescence quantum yield could be determined as a result of the poor film obtained for **4cc**.

Among the polymers having 2-ethylhexyloxy side groups, **4dd** ($\lambda_{max,\ abs}$ = 459 and 482 nm, $\lambda_{max,em}$ = 584 nm), with both R^2 and R^4 equal to 2-ethylhexyloxy, has the largest Stokes shift (83 nm) and the lowest photoluminescence quantum yield (24%) (Figure 10). However its Stokes shift is smaller than those of **4cc** and **4ac** and its emission spectrum is narrower, indicative of lesser excimers formation. The absorption curves of **4ad** and **4da** consist of peaks with double maxima; $\lambda_{max,\ abs}$ = 459 and 478 nm for **4ad** and $\lambda_{max,\ abs}$ = 465 and 482 nm. The structured emission spectrum of **4ad** is made up of two maxima, one less intensive at $\lambda_{max,em}$ = 512 nm and one more intensive at $\lambda_{max,em}$ = 539 nm, showing a Stokes shift of 61 nm and fluorescence quantum yield of 44%. Exchanging the position of the side chains from **4ad** to **4da** gives rise to an exchange of the peaks intensity of the emission curve. The emission trace of **4da** is namely characterized with a maximum at $\lambda_{max,em}$ = 515 nm and a shoulder at 538 nm, leading to a Stokes shift of 33 nm (which is almost half of that of **4ad**) and a fluorescence quantum yield of 31%. The relatively (to **4ad**) smaller Stokes shift and narrower fluorescence spectrum of **4da** once more confirms the fact that longer side chains at position R^4 hinder strong excimers formation. This is furthermore illustrated in Figure 11, where the absorption and emission spectra of polymer **5a** and **5c** in the solid state are depicted.

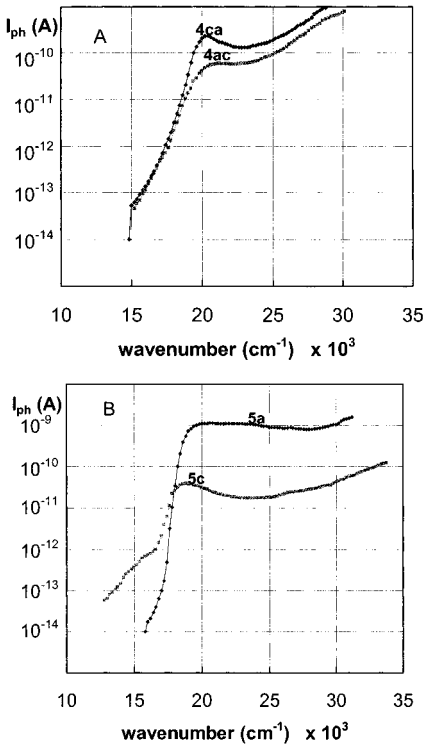

Figure 6. Photoconductivity spectra of **4ac** and **4ca** and of **5a** and **5c** (surface type cell, slit width 0.2 mm, light intensity 20 μW, threshold voltage 400 (A) or 10 V (B)).

Table 4. Data from the Absorption Spectra in Chloroform Solution and in the Solid State of Monomers 1c,d, 10c,d, 2, and 15 and Polymers 4 and 5

compound	λ_{max}/nm	ϵ/M^{-1} cm^{-1}	$\lambda_{0.1max}$/nm	E_g^{opt}/eV[a]
1c	393	41 700	442	2.80
10c	410	68 200	459	2.68
1d	399	40 600	450	2.75
10d	421	64 500	473	2.62
2	421	60 750	478	2.59
15	409	60 300	472	2.62
4ba	448	100 000[b]	488	2.54
4ba[c]	455, 477		492	2.52
4ac	446	94 000[b]	490	2.53
4ac[c]	465		503	2.46
4ca	446	104 200[b]	490	2.53
4ca[c]	454, 483		489	2.53
4 cm^3	445	85 100	490	2.53
4 cm^3[c]	459, 482		500	2.48
4dd	450	108 300[b]	492	2.53
4dd[c]	454		488	2.54
4ad	450	110 080[b]	491	2.53
4ad[c]	459, 478		496	2.50
4da	448	98 560[b]	492	2.53
4da[c]	464:sh, 483		501	2.47
5a	468	86 300[b]	521	2.38
5a[c]	498		541	2.29
5c	472	101 160[b]	520	2.40
5c[c]	491		522	2.37

[a] $E_g^{opt} = hc/\lambda_{0.1max}$. [b] Per mole of repeating unit. [c] Solid state.

Similar to the solution, **5a** and **5c** absorb and fluoresce in film at longer wavelengths than polymers of type **4** due to their higher number of side chains. Polymer **5a** has its absorption band centered at $\lambda_{max,abs}$ = 498 nm; that of **5c** is 7 nm blue shifted and is found at $\lambda_{max,abs}$ = 491 nm, as a result of a greater nonplanar conformation of the conjugated backbone in **5c** than in

Table 5. Photoluminescence Data of the New Compounds in Dilute $CHCl_3$ Solution and in Solid State

compound	$\lambda_{max,\,exc}$/nm	$\lambda_{max,\,em}$/nm	Stokes shift/nm	ϕ_{fl}/%
1c	395	462	67	83
10c	412	463 (sh: 499)	51	77
1d	398	463	65	83
10d	421	468 (sh: 501)	47	71
2	423	466	43	73
15	408	470	62	59
4ba	448	489 (sh: 522)	41	76
4ba[a]	454, 477	508, 541	31	25
4ac	450	490 (sh: 520)	40	68
4ac[a]	465	602	137	19
4ca	449	489 (sh: 520)	40	78
4ca[a]	455, 483	510, 544	27	29
4 cm3	444	490 (sh: 521)	46	76
4 cm3 [a]	459	584	125	–
4dd	450	491 (sh: 525)	41	70
4dd[a]	455	538	83	24
4ad	451	490 (sh: 521)	39	74
4ad[a]	461, 478	512, 539	61	44
4da	450	490 (sh: 525)	40	75
4da[a]	465, 482	515 (sh: 538)	33	31
5a	472	519 (sh: 560)	47	77
5a[a]	496	552, 592	56	54
5c	472	519 (sh: 560)	47	70
5c[a]	491	553, 591	62	29

[a] Solid state.

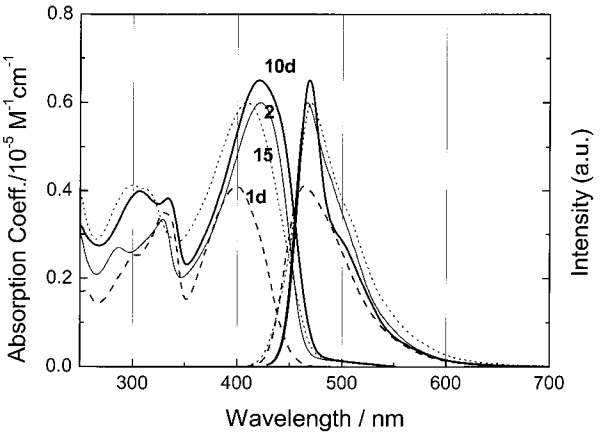

Figure 7. Absorption and normalized emission spectra of monomers **1d**, **10d**, **2**, and **15** in dilute chloroform solution.

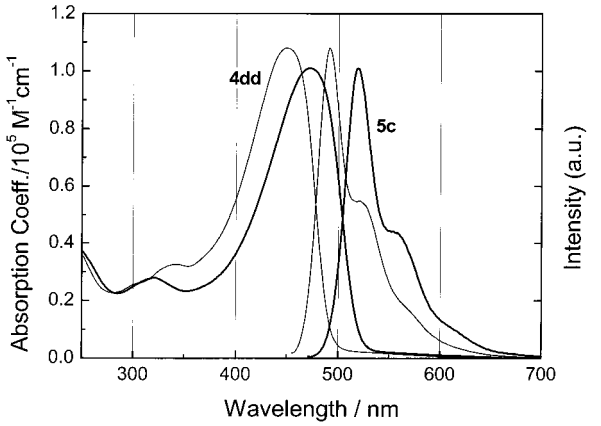

Figure 8. Absorption and normalized emission spectra of polymers **4dd** and **5c** in dilute chloroform solution.

5a. While the emission trace of **5c** ($R^4 = O(CH_2)_7CH_3$) is slightly structured and broader with two maxima of almost identical intensity at $\lambda_{max,em} = 553$ nm and $\lambda_{max,em} = 591$ nm, showing a Stokes shift of 62 nm and a fluorescence quantum yield of 29%, the emission spectrum of **5a** ($R^4 = O(CH_2)_{17}CH_3$) is well structured and narrower. Its peak at $\lambda_{max,em} = 552$ nm is greatly more intense than that at $\lambda_{max,em} = 591$ nm. A Stokes shift of 56 nm and a fluorescence quantum yield of 54% were obtained. The structure of the emission curve and the very high ϕ_{fl} value of **5a** are indications of the fact that its conjugated backbone behave as if it was *dissolved* in a hydrocarbon solvent chain,[28] thus strongly hindering $\pi-\pi$ interchain interactions in the ground state and subsequently excimers formation in the excited state.

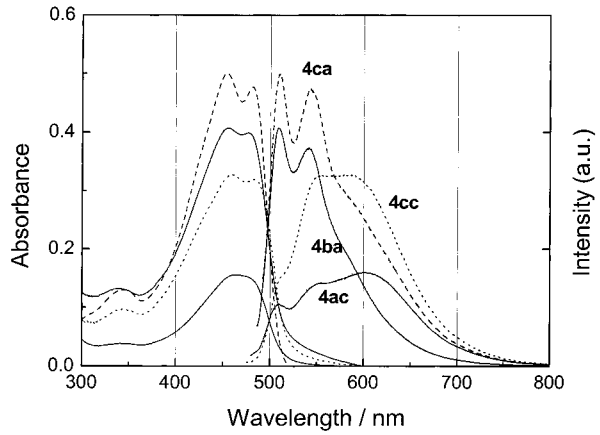

Figure 9. Solid-state absorption and normalized emission spectra of polymers **4ba**, **4cc**, **4ac**, and **4ca**.

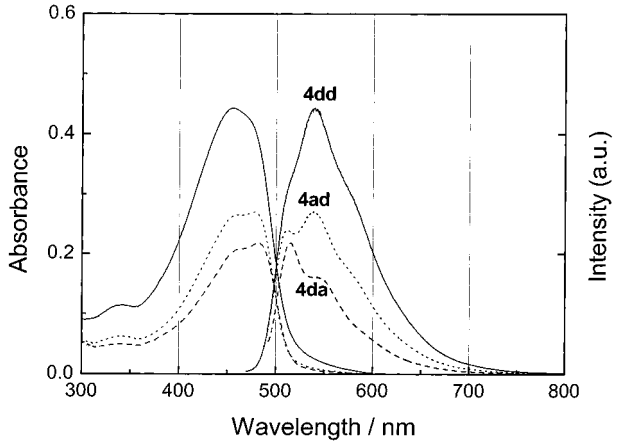

Figure 10. Solid-state absorption and normalized emission spectra of polymers **4dd**, **4ad**, and **4da**.

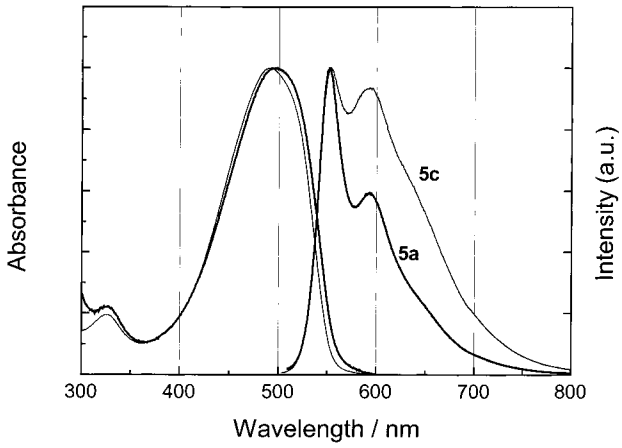

Figure 11. Normalized solid-state absorption and emission spectra of polymers **5a** and **5c**.

Wide-angle and small-angle X-ray scatterings investigations for a better understanding of the long range order in solid state and the detailed study of photophysics of the new compounds are under way and will be published in the nearest future.

Experimental Section

Materials. All starting materials were purchased from Fluka. Toluene was dried and distilled over sodium and benzophenone. DMSO was dried over molecular sieve and distilled. Diisopropylamine was dried and distilled over KOH. The solvents were degassed by flushing with argon 1 h prior to use.

Measurements. Mass spectroscopy was performed by chemical ionization with H_2O vapor as gas on a Finnigan Mat SSQ 710. ^{1}H NMR and ^{13}C NMR were measured in deuterated chlorofrom on a Bruker DRX 400 and a Bruker AC 250 using tetramethylsilane as internal standard. The elemental analysis was performed on a CHNS-932 Automat Leco. Gel permeation chromatography (GPC) was performed on a set of Knauer, using THF as eluent and polystyrene as standard. The absorption spectra were recorded on a Perkin-Elmer UV/vis−NIR spectrometer Lambda 19. Quantum-corrected emission spectra were measured in dilute chloroform solution with an LS 50 luminescence spectrometer (Perkin-Elmer). Photoluminescence quantum yields were calculated according to Demas and Crosby[31] against quinine sulfate in 0.1 N sulfuric acid as standard ($\phi_{fl} = 55\%$). The solid-state absorption and emission were measured using Hitachi F-4500. The films were spin-casted from a chlorobenzene solution. The quantum yield in solid state was determined against a CF_3P−PPV copolymer reference which has been measured by an integrating sphere to be 0.43. Infrared spectroscopy was recorded on a Nicolet Impact 400. A homemade apparatus served for thermogravimetry measurements. The measurements were done under ambient atmosphere while heating at a rate of 10 K/min. Electrochemical measurements were carried out with a Princeton Research PAR 273 A instrument [Pt disk electrode, CH_2Cl_2, (TBA)PF_6, concentrated 10^{-3} mol/L, sweep rate 0.02 V/s (DPP), 0.167 V/s (CV)]. DSC was obtained using Perkin-Elmer DSC 2C, while heating or cooling at a rate of 10 K/min. Polarized optical microscopy (POM) investigations were conducted on a Carl-Zeiss Axiopol microscope equipped with a Linkam THMS 600 hot stage CI-93 controller. For investigation of thermotropic mesomorphism, small amounts of sample compound were dissolved in a minimum amount of dichloromethane. The solution was placed between two glass slides and the solvent was allowed to evaporate gradually. For detection of lyotropic mesophases, a thin film of sample compound was placed between a glass side and a coverslip and small amounts of solvent were added dropwise, allowing a gradual change in solvent concentration. All studies were carried out with crossed polarizers.

1,4-Bis((2-ethylhexyl)oxy)benzene (6).[19] A suspension of KOH powder (48.0 g, 0.856 mol) in dried DMSO (200 mL) was stirred and degassed for 1 h. Hydroquinone (11.02 g, 0.1 mol) and 2-ethylhexyl bromide (76.0 g, 0.394 mol) were then added. The reaction mixture was stirred for 3 h at room temperature and finally poured into ice water (600 mL). The organic layer was collected and the aqueous layer was extracted with hexane (3 × 200 mL). The combined organic layers were dried over $MgSO_4$, and the solvent was evaporated to give a yellow oil, which was distilled under reduced pressure to yield a colorless liquid (26.0 g, 77.71%). Bp: 165 °C (0.05 Torr). ^{1}H NMR (250 MHz, $CDCl_3$): δ/ppm = 0.96−1.77 (30H, $-CH(CH_2CH_3)(CH_2)_3CH_3$), 3.90 (4H, $-CH_2O-$), 6.89 (4H, $C_{aryl}-H$). ^{13}C NMR (62 MHz, $CDCl_3$): δ/ppm = 11.49 (CH_3−ethyl), 14.47 (CH_3− hexyl), 23.46, 24.27, 29.49, 30.94, (−CH_2− ethyl and hexyl), 39.88 (−CH−), 71.64 (−CH_2O-), 115.78 ($C_{aryl}-H$), 153.86 ($C_{aryl}-OR$). Anal. Calcd for $C_{22}H_{38}O_2$ (334.54): C, 78.99; H, 11.45. Found: C, 78.80; H 11.50.

1,4-Bis(trimethylsilylethynyl)-2,5-bis((2-ethylhexyl)-oxy)benzene (8). 1,4-Diiodo-2,5-bis(2-ethylhexyloxy)benzene (**7**)[19] (6.5 g, 11.0 mmol), $Pd(PPh_3)_2Cl_2$ (385 mg, 0.55 mmol), and CuI (105 mg, 0.55 mmol) were dissolved in 100 mL of dried and degassed diisopropylamine. Trimethylsilylacetylene (3.24 g, 33.0 mmol) was added dropwise to the vigorously stirred solution. The reaction mixture was then stirred at reflux for 3 h. After cooling, toluene (200 mL) was added, and the white ammonium iodide precipitate was filtered off. The solvent was removed on a rotary evaporator; the remaining oil was dissolved in toluene and passed through a 4 cm plug of silica gel. The evaporation of the solvent led a brown oil (yield: 6.82 g, 76.78%).^{1}H NMR (250 MHz, $CDCl_3$): δ/ppm = 0.058 (18H, $-Si(CH_3)_3$), 0.74 (12H, $-CH_3$), 1.10−1.96 (18H, −CH− and $-CH_2-$), 3.64 (4H, $-CH_2O-$), 6.69 (2H, $C_{aryl}-H$). ^{13}C NMR (62 MHz, $CDCl_3$): δ/ppm = −0.00 ($-Si(CH_3)_3$), 11.33 (CH_3− ethyl), 14.16 (CH_3− hexyl), 23.13, 23.95, 29.76, 30.69 ($-CH_2-$), 39.97 (−CH−), 71.70 ($-CH_2O-$), 99.88, 101.19 (−C≡C−), 113.84 ($C_{phenyl}-C\equiv$), 116.78 ($C_{phenyl}-H$), 154.21 ($C_{phenyl}-OR$).

1,4-Diethynyl-2,5-bis(2-ethylhexyloxy)benzene (9). Methanol (112 mL) and aqueous KOH (8 mL, 20%) were added at room temperature to a stirred solution of 1,4-bis(trimethylsilylethynyl)-2,5-bis(2-ethylhexyloxy)benzene (6.66 g, 12.6 mmol) in THF (220 mL). After stirring for 2 h, the solvent was evaporated and the residual oil was stirred at reflux with charcoal in hexane. After cooling, filtration and evaporation of the solvent, it was chromatographed on a silica gel column with toluene as eluent. 4.3 g of a dark red oil was obtained, which was used without further purification. Yield: 89.56%. ^{1}H NMR (250 MHz, $CDCl_3$): δ/ppm = 0.82−1.69 (30H, $CH_3(CH_2)CH(CH_2CH_3)-$), 3.25 (2H, −C≡C−H), 3.77 (4H, $-CH_2O-$), 6.92 (2H, $C_{phenyl}-H$). ^{13}C NMR (62 MHz, $CDCl_3$): δ/ppm = 11.54 (CH_3− ethyl), 14.47 (CH_3− hexyl), 23.43, 24.34, 29.44, 30.97 ($-CH_2-$), 39.75 (−CH−), 72.58 ($-CH_2O-$), 82.69, 83.21 (−C≡C−), 113.62 ($C_{phenyl}-C\equiv$), 117.91 ($C_{phenyl}-H$), 154.64 ($C_{phenyl}-OR$).

1,4-Bis(4-formylphenylethynyl)-2,5-bis((2-ethylhexyl)-oxy)benzene (1d) and 1,4-Bis[4-formylphenylethynyl-(2,5-bis((2-ethylhexyl)oxy)phenyl)]-buta-1,3-diyne (10d). 1,4-Diethynyl-2,5-bis(2-ethylhexyloxy)benzene (**9**) (4.0, 10.45 mmol), 4-bromobenzaldehyde (5.803 g, 31.36 mmol), $Pd(PPh_3)_4$ (483 mg, 0.42 mmol), and CuI (80 mg, 0.38 mmol) were put into to a degassed solution of 100 mL of diisopropylamine and 200 mL of toluene. The reaction mixture was heated at 70−80 °C for 24 h while bubbling the solution with argon. After the reaction was cooled to room temperature, the precipitated diisopropylammonium bromide was filtered off and the solvent was distilled off under vacuum. The residue was chromatographed on a silica gel column with toluene as eluent. **1d** was obtained at $R_f = 0.34$ (4.152 g, 67.25%) and **10d** at $R_f = 0.41$ (80 mg, 0.78%).

1d. Mp = 112−114 °C. MS: m/z = 591 (M +1, basepeak), 479 (15%), 366 (45%), 185 (10%).

^{1}H NMR (250 MHz, $CDCl_3$): δ/ppm = 0.88−EnDash1.88 (30H, m, $CH_3(CH_2)_3CH(CH_2CH_3)-$), 3.95 (4H, d, ^3J = 6.52 Hz, $-CH_2O-$), 7.06 (2H, s, $C_{aryl}-H$), 7.68 (4H, d, ^3J = 8.20 Hz, $C_{aryl}-H$), 7.90 (4H, d, ^3J = 8.25 Hz, $C_{aryl}-H$), 10.04 (2H, s, CHO). ^{13}C NMR (62 MHz, $CDCl_3$): δ/ppm = 11.68, 14.06 (CH_3-), 23.46, 24.43, 29.55, 30.99, 31.09 ($-CH_2CH(CH_2)_3-$), 72.38 ($-CH_2O-$), 90.53, 94.59 (−C≡C−), 114.25 ($C_{aryl}-C\equiv C-$), 116.92 ($C_{aryl}-H$), 129.98 ($C_{aryl}-C\equiv C-$), 130.13, 132.37 ($C_{aryl}-H$), 135.81 ($C_{aryl}-CHO$), 154.47 ($C_{aryl}-OR$), 191.73 (−CHO). IR (KBr): 3061 (w, $C_{aryl}-H$) 2951, 2928, 2863 (vs, CH_2 and CH_3), 2736 (m, −CHO), 2207 (s, disubst −C≡C−), 1697 (s, −CHO), 1600 (s, $-C=C-_{aryl}$), 1217 (vs, $C_{aryl}-OR$) cm^{-1}. UV−vis ($CHCl_3$): λ_{max}/nm (ϵ/(M^{-1} cm^{-1})) 254.4 (16 970), 302.4 (25 067), 329.6 (34 642), 399.2 (41 700). Anal. Calcd for $C_{40}H_{46}O_4$ (590.80): C, 81.31;H, 7.84. Found: C, 80.81; H, 7.79.

10d. MS: m/z = 971 (M+1, 70%), 263 (basepeak), 185 (99%). ^{1}H NMR (400 MHz, $CDCl_3$): δ/ppm = 0.78−1.72 (60H, m, $CH_3(CH_2)_3CH(CH_2CH_3)-$), 3.81 (8H, $-CH_2O-$), 6.92 (2H, $C_{aryl}-H$), 7.00 (2H, $C_{aryl}-H$), 7.57 (4H, d, ^3J = 8.05 Hz, $C_{aryl}-H$), 7.78 (4H, d, ^3J = 8.05 Hz, $C_{aryl}-H$), 9.94 (2H, s, CHO). ^{13}C NMR (100 MHz, $CDCl_3$): δ/ppm = 11.56, 11.65, 14.45, 14.50 (CH_3-), 23.08, 23.45, 24.38, 24.42, 29.51, 29.75, 30.09, 30.99, 31.08, 32.32, 39.73, 39.79, 39.97 ($-CH_2CH(CH_2)_3-$), 72.36, 72.67 ($-CH_2O-$), 80.01, 80.21 (−C≡C−C≡C−), 90.52, 94.79 (−C≡C−), 113.86, 114.07, 114.47 ($C_{aryl}-C\equiv C-$), 117.16, 117.66,

117.88 (C_{aryl}−H), 128.72, 129.97 (C_{aryl}−C≡C−), 130.12, 132.37 (C_{aryl}−H), 134.46, 135.82 (C_{aryl}−CHO), 154.36, 155.46, 155.58 (C_{aryl}−OR), 191.72 (CHO). IR (FTIR): 3053 (w. C_{aryl}−H) 2957, 2923, and 2856 (vs, CH_2 and CH_3), 2729 (w, CHO), 2208 (m, disubst −C≡C−), 2143 (w, −C≡C−C≡C−) 1700 (vs, CHO), 1599 (vs, −C═C−$_{aryl}$), 1215 and 1206 (vs, C_{aryl}−OR) cm^{-1}. UV−vis ($CHCl_3$): λ_{max}/nm (ϵ/(M^{-1} cm^{-1})) 305.4 (8180), 333.6 (7855), 420.8 (13 130).

1,4-Bis(bromomethyl)-2,5-bis((2-ethylhexyl)oxy)benzene (11). A suspension of **6** (15 g, 44.84 mmol), paraformaldehyde (18.55 g, 614.84 mmol), and NaBr (23.10 g, 222.61 mmol) in glacial acetic acid (130 mL) was heated at 60 °C. A 1:1 mixture of concentrated sulfuric acid and glacial acetic acid (53 mL) was added dropwise, and the reaction mixture was stirred for 4 h at 70 °C. After the reaction was cooled at 0 °C, the precipitate was filtered off, washed with water, and recrystallized from hexane. 16.0 g (87.45%) of white solid was obtained. Mp: 63−64 °C. ^{1}H NMR (400 MHz, $CDCl_3$): δ/ppm = 0.915−2.19 (30H, m, $CH_3(CH_2)_3CH(CH_2CH_3)$−), 3.90 (4H, t, $3J$ = 5.36 Hz, $-CH_2O-$), 4.55 (4H, s, $-CH_2Br$), 6.88 (2H, s, C_{aryl}−H). ^{13}C NMR (100 MHz, $CDCl_3$): δ/ppm = 11.63, 14.47 (CH_3−), 23.44, 24.43, 29.51, 31.04, 40.02 ($-CH_2CH(CH_2)_3-$), 29.11 ($-CH_2Br$), 71.38 ($-CH_2O-$), 114.66 (C_{aryl}−H), 127.80 (C_{aryl}−CH_2Br), 151.12 (C_{aryl}−OR). Anal. Calcd for $C_{24}H_{40}Br_2O_2$ (520.38): C, 55.39; H, 7.74; Br, 30.70. Found: C, 55.49;H,7.82; Br, 30.97.

2,5-Bis((2-ethylhexylo)xy)-*p*-xylylene-bis(diethylphosphonate) (3d). A mixture of **11** (16.0, 30.72 mmol) and an excess of triethyl phosphite (15.3 g, 92.2 mmol) was heated slowly to 150−160 °C, and the evolving ethyl bromide was distilled off simultaneously. After 4 h, vacuum was applied for 1 h at 180 °C to remove the excess triethyl phosphite. The resulting oil was dried under reduced pressure. It solidified when kept under 18 °C. Yield: 19.5 g (99.91%). Mp: 18−20 °C. ^{1}H NMR (250 MHz, $CDCl_3$): δ/ppm = 0.87−1.71 (42H, m, CH_3−ethyl and $CH_3(CH_2)_3CH(CH_2CH_3)$−), 3.22 (4H, d, $3J$ = 20.12 Hz, $-CH_2P$), 3.81 (4H, t, $3J$ = 5.54 Hz, $-CH_2O-$ ethyhexyl), 3.95 (8H, m, $-CH_2O-$ ethyl), 6.94 (2H, s, C_{aryl}−H). ^{13}C NMR (62 MHz, $CDCl_3$): δ/ppm = 11.52, 14.14 (CH_3− ethylhexyl), 16.66 (CH_3−ethyl), 23.41, 24.30, 25.44, 27.64, 29.50, 30.99, 40.07 ($-CH_2CH(CH_2)_3-$), 62.19 ($-CH_2O-$ethyl), 71.60 ($-CH_2O-$ethylhexyl), 115.09 (C_{aryl}−H), 119.74 (C_{aryl}−CH_2P), 150.8 (C_{aryl}−OR). Anal. Calcd for $C_{32}H_{60}P_2O_8$ (634.77): C, 60.54; H, 9.52. Found: C, 60.27; H, 9.67.

1-Bromo-4-formyl-2,5-dioctyloxybenzene (13). To a solution of 1,4-dibromo-2,5-dioctyloxybenzene (**12**)[23a] (4.9 g, 10 mmol) in diethyl ether (150 mL), cooled at 10 °C and kept under argon, was added a solution of butyllithium (2.7 M in heptane, 3.75 mL, 10 mmol). After 15 min, DMF (0.96 mL, 12.5 mmol) was added to the mixture, while the temperature was allowed to rise to 15 °C. The clear solution was kept between 10 and 15 °C and was stirred for 1.5 h. A 10% aqueous HCl solution (50 mL) was subsequently added to the mixture, and the phases were separated. The organic phase was washed with a $NaHCO_3$ solution and dried over $CaCl_2$. Diethyl ether was then distilled off, and the residue was recrystallized from methanol. Thus 2.7 g (61%) of light yellow crystals was obtained. Mp: 62−63 °C. ^{1}H NMR (250 MHz, $CDCl_3$): δ/ppm = 0.81−1.79 ($CH_3(CH_2)_6$−), 3.80−4.0 ($-CH_2O-$), 7.03 and 7.35 (C_{aryl}−H), 10.39 (CHO). ^{13}C NMR (62 MHz, $CDCl_3$): δ/ppm = 14.45, 14.46, 23.02, 26.31, 26.37, 29.39, 29.44, 29.58, 29.62, 32.14, 32.16 ($CH_3(CH_2)_6$−), 69.85 and 70.22 ($-CH_2O-$), 111.01 and 118.84 ($-C_{aryl}$−H), 121.34 ($-C_{aryl}$−Br), 124.65 ($-C_{aryl}$−CHO), 150.24 and 156.15 (C_{aryl}−OR), 189.33 (−CHO). Anal. Calcd for $C_{23}H_{37}BrO_3$ (441.46): C, 62.57; H, 8.44; Br, 18.09. Found: C, 62.68; H,8.55; Br, 18.40.

1,4-Bis(4-formyl-2,5-dioctyloxyphenylethynyl)-2,5-dioctadecyloxybenzene (2) and 1,4-Bis[4-formyl-2,5-dioctyloxyphenylethynyl-(2,5-dioctadecyloxyphenyl)]buta-1,3-diyne (15). 1,4-Diethynyl-2,5-dioctadecylbenzene (**14**) [23a] (2.1 g, 3.167 mmol), 1-bromo-4-formyl-2,5-dioctyloxybenzene (**13**) (3.062 g, 6.9362 mmol), $Pd(PPh_3)_4$ (146 mg, 0.126 mmol, 4 mol %), and CuI (26 mg, 0.126 mmol, 4 mol %) were added to a degassed solution of 40 mL of diisopropylamine and 90 mL of toluene. The reaction mixture was heated at 70 to 80 °C for 24 h. After being cooled to room temperature, it was added dropwise into 500 mL of vigorously stirred methanol. The precipitate was collected and chromatographed on a silica gel column with toluene/hexane as eluent. **2** was obtained at R_f = 0.45 (2.7 g, 60%) and **15** at R_f = 0.75 (200 mg, 3%).

2. Mp: 103−103.5 °C. MS(70 eV, ESI in CH_2Cl_2 + CH_3-OH): m/z = 1405 (M +Na, 100%).

^{1}H NMR (400 MHz, $CDCl_3$): δ/ppm = 0.85 (18H, m, CH_3−), 1.21−1.83 (112H, m, $-(CH_2)_6-$ and $-(CH_2)_{16}-$), 4.02 (12H, m, $-CH_2O-$), 7.00 (2H, s, C_{phenyl}−H), 7.08 (2H, s, C_{phenyl}−H), 7.30 (2H, s, C_{phenyl}−H), 10.43 (2H, s, −CHO). ^{13}C NMR (100 MHz, $CDCl_3$): δ/ppm = 14.04, 14.07 (CH_3−), 22.62, 22.63, 22.66, 29.20, 29.28, 29.30, 29.33, 29.34, 29.63, 29,68, 31.81, 31.90 ($-(CH_2)_6-$ and $-(CH_2)_{16}-$), 69.24, 69.43, 69.72 ($-CH_2O-$), 91.17, 93.78 (−C≡C−), 110.14 (C_2), 114.37 (C_7), 117.37 (C_5), 117.55 (C_8), 120.69 (C_4), 124.93 (C_1), 153.59, 153.69 (C_3 and C_9), 155.49 (C_6), 189.07 (CHO). IR (KBr): 3075 (w, C_{phenyl}−H), 2922 and 2851 (vs, $-CH_2-$ and CH_3), 2755 (w, CHO), 2201 (w, disubst −C≡C−), 1682 (s, CHO), 1598 (s, −C═C−$_{phenyl}$), 1220 (s, C_{phenyl}−OR) cm^{-1}. UV−vis ($CHCl_3$): λ_{max}/nm (ϵ/(M^{-1} cm^{-1})) 286.4 (29 000), 328.8 (35 200), 421.6 (60 750). Anal. Calcd for $C_{92}H_{150}O_8$ (1384.19): C, 79.83;H, 10.92. Found: C, 79.96; H, 10.45.

15. MS (70 eV, ESI in CH_2Cl_2 + CH_3OH): m/z = 1021 (M/2, 80%), 685 (100%), 324 (78%). ^{1}H NMR (400 MHz, $CDCl_3$): 0.83−1.81 (200H, m, $-(CH_2)_6-$ and $-(CH_2)_{16}-$), 3.86−4.04 (16H, m, $-CH_2O-$), 6.79−7.29 (8H, C_{phenyl}−H), 10.420 and 10.426 (2H, −CHO).

^{13}C NMR (100 MHz, $CDCl_3$): δ/ppm = 14.10, 14.12, 22.66, 22.69, 25.94, 26.09, 29.14, 29.19, 29.23, 29.32, 29.46, 29.67, 29.71, 31.80, 31.84, 31.92 ($CH_3(CH_2)_{16}-$ and $CH_3(CH_2)_6-$), 68.67, 69.15, 69.37, 69.72, 69.82 ($-CH_2O-$), 79.52, 79.59 (−C≡C−C≡C−), 89.26, 91.52, 93.68 (−C≡C−), 109.99, 113.09, 113.32, 114.18, 114.78, 117.07, 117.12, 117.47, 117.75, 118.60, 120.55, 121.09, 124.76, 124.87 (C_{phenyl}'s), 152.81, 153.49, 153.56, 153.66, 154.13, 154.93, 155.47 (C_{phenyl}−OR), 189.17 (CHO). IR (KBr): 3075 (w, C_{phenyl}−H), 2922 and 2851 (vs, $-CH_2-$ and CH_3), 2756 (w, CHO), 2201 (w, disubst. −C≡C−), 2152 (w, −C≡C−C≡C−), 1683 (s, CHO), 1601 (s, −C═C−$_{phenyl}$), 1219 (s, C_{phenyl}−OR) cm^{-1}. UV−vis ($CHCl_3$): λ_{max}/nm (ϵ/(M^{-1} cm^{-1})) 299.2 (42 220), 312.2 (49 600), 408.8 (60 325). Anal. Calcd for $C_{138}H_{226}O_{10}$ (2045.30): C, 81.04; H, 11.13. Found: C, 80.94; H, 11.36.

Poly[1,4-phenyleneethynylene-1,4-(2,5-dioctyloxyphenylene)-1,4-phenyleneethene-1,2-diyl-1,4-(2,5-dioctadecyloxyphenylene)ethene-1,2-diyl] (4ca). Dialdehyde **1c** (1.0 g, 1.69 mmol) and bisphosphonate **3a** (1.549 g, 0.75 mmol) were dissolved in dried toluene (50 mL) while stirring vigorously under argon and heating under reflux. Potassium *tert*-butoxide (759 mg, 6.79 mmol) was added to this solution. After 30 min, additional toluene (50 mL) was added and the reaction mixture was heated at reflux for 2 h. After this time more toluene was added and the reaction was quenched with aqueous HCl. The organic phase was separated and extracted several times with distilled water until the water phase became neutral (pH = 6−7). The organic layer was dried in a Dean−Stark apparatus. The resulting toluene solution was filtered, evaporated under vacuum to the minimum and precipitated in methanol. The polymer was extracted 8 h with methanol, dissolved once more in toluene, reprecipitated in methanol and dried under vacuum. 1.4 g (69.15%) of yellow polymer was obtained. GPC (THF): $\bar{M}_w$ = 156 900, $\bar{M}_n$ = 50 060, polydispersity index = 3.1. ^{1}H NMR (250 MHz, $CDCl_3$): δ/ppm = 0.80−1.79 ($CH_3(CH_2)_{16}$ and $CH_3(CH_2)_6$−), 3.97 ($-OCH_2-$), 6.95−7.49 (aromatic and vinylene H's). ^{13}C NMR (62 MHz, $CDCl_3$): δ/ppm = 14.50, 23.08, 26.55, 30.09, 32.29 ($CH_3(CH_2)_{16}$ and $CH_3(CH_2)_6$−), 70.05 ($-OCH_2-$), 95.64 (−C≡C−), 111.12, 117.36, 132.28 (C_{phenyl}−H), 126.82 (−CH═CH−), 114.50, 122.61, 124.78, 128.65, 138.31 (C_{phenyl}−C), 151.62, 154.07 (C_{phenyl}−OR). IR(KBr): 3056 (w, C_{phenyl}−H), 2923 and 2851 (vs, CH_3 and $-CH_2-$), 2201 (vw, −C≡C−), 1625 (s, aromatic−C═C−),1211 (s, C_{aryl}−OR), 967 (m, trans−CH═CH−) cm^{-1}. UV−vis ($CHCl_3$): λ_{max}/nm (ϵ/(M^{-1} cm^{-1})) 344 (29 100), 446.0 (104 200). Anal. Calcd for $(C_{84}H_{124}O_6)_n$ $(1197.90)_n$: C, 84.22;H, 10.43. Found: C, 82.96; H,11.04.

Poly[1,4-phenyleneethynylene-1,4-(2,5-didodecyloxyphenylene)-1,4-phenyleneethene-1,2-diyl-1,4-(2,5-dioctadecyloxyphenylene)ethene-1,2-diyl] (4ba). Dialdehyde **1b** (1.0 g, 1.42 mmol) and bisphosphonate **3a** (1.302 g, 1.42 mmol) were dissolved in dried toluene (50 mL) while stirring vigorously under argon and heating under reflux. Potassium *tert*-butoxide (480 mg, 4.27 mmol) was added to this solution. After 30 min, 30 mL of toluene was added, and the reaction mixture was heated at reflux in total for 1 h 30 min. After this time, more toluene was added and the reaction was quenched with aqueous HCl. The workup was done as described above. Thus 1.633 g (87.77%) of yellow polymer was obtained.

GPC(THF): $\bar{M}_n$ = 39 200, $\bar{M}_w$ = 166 600, polydispersity index = 4.2.

^{1}H NMR (250 MHz, $CDCl_3$): δ/ppm = 0.84−1.87(116H, CH_3-$(CH_2)_{10}$ and $CH_3(CH_2)_{16}$−), 4.04 (8H, $-OCH_2-$), 7.00−7.49 (16H, aromatic and vinylene H's). ^{13}C NMR (62 MHz, $CDCl_3$): δ/ppm = 14.08, 22.62, 26.07, 26.26, 29.31, 29.39, 29.64, 31.06 ($CH_3(CH_2)_{10}$- and $CH_3(CH_2)_{16}$−), 69.69 ($-OCH_2-$), 110.69, 116.96, 131.86 (C_{phenyl}−H), 126.36 (−CH=CH−), 128.65, (C_{phenyl}−C), 151.22, 153.66 (C_{phenyl}−OR). IR(KBr): 3053 (w, C_{phenyl}−H), 2920 and 2851 (vs, CH_3 and $-CH_2-$), 2209 (vw, disubst −C≡C−), 1599 (s, aromatic −C=C−),1211 (s, C_{aryl}−OR), 965 (m, *trans*-CH=CH−) cm^{-1}. UV−vis ($CHCl_3$): λ_{max}/nm (ϵ/(M^{-1} cm^{-1})) 301.6, 341.6, 448.0 (100 046). Anal. Calcd for $(C_{92}H_{140}O_4)_n$ (1310.12)$_n$: C, 84.34; H,10.77. Found: C, 84.49; H, 10.44.

Poly[1,4-phenyleneethynylene-1,4-(2,5-di(2-ethylhexyloxy)phenylene)-1,4-phenyleneethene-1,2-diyl-1,4-(2,5-di(2-ethylhexyloxy)phenylene)ethene-1,2-diyl] (4dd). Dialdehyde **1d** (1.004 g, 1.70 mmol) and bisphosphonate **3d** (1.079 g, 1.79 mmol) were dissolved in dried toluene (50 mL) while stirring vigorously under argon and heating under reflux. Potassium *tert*-butoxide (760 mg, 6.79 mmol) was added to this solution. After 30 min, 30 mL of toluene was added and the reaction mixture was heated at reflux in total for 1 h 30 min. After this time more toluene was added and the reaction was quenched with aqueous HCl. The workup was done as described above. 859 mg (55.08%) of yellow polymer was obtained. GPC (THF): $\bar{M}_n$ = 35 240, $\bar{M}_w$ = 161 700, polydispersity index = 4.5. ^{1}H NMR (250 MHz, $CDCl_3$): δ/ppm = 0.94−1.85 (60H, $-CH(CH_2CH_3)(CH_2)_3-$), 3.98 (8H, $-OCH_2-$), 7.05−7.53 (16H, aromatic and vinylene H's). ^{13}C NMR (62 MHz, $CDCl_3$): δ/ppm = 11.70,(CH_3−ethyl) 14.49 (CH_3−hexyl), 23.50, 24.42, 29.60, 31.06 ($-CH_2-$ethyl and $-(CH_2)_3-$hexyl), 40.14 (−CH−), 72.44 ($-OCH_2-$), 110.78, 116.99, 132.23 (C_{phenyl}−H), 126.74 (−CH=CH−). IR(KBr): 3036 (w, C_{phenyl}−H), 2922 and 2850 (vs, CH_3 and $-CH_2-$), 2209 (vw, disubst −C≡C−), 1596 (s, aromatic C=C−),1211 (s, C_{aryl}−OR), 965 (m, *trans*-CH=CH−) cm^{-1}. UV−vis ($CHCl_3$): λ_{max}/nm (ϵ/(M^{-1} cm^{-1})) 303.6, 342.4 (32 700), 449.0 (108 317). Anal. Calcd for $(C_{64}H_{84}O_4)_n$ (917.36)$_n$: C, 83.79; H, 9.22. Found: C, 79.48; H, 9.53.

Poly[1,4-phenyleneethynylene-1,4-(2,5-dioctadecyloxyphenylene)-1,4-phenyleneethene-1,2-diyl-1,4-(2,5-di-(2-ethylhexyloxy)phenylene)ethene-1,2-diyl] (4ad). Dialdehyde **1a** (906 mg, 1.04 mmol) and bisphosphonate **3d** (660 mg, 1.04 mmol) were dissolved in dried toluene (50 mL) while stirring vigorously under argon and heating under reflux. Potassium *tert*-butoxide (467 mg, 4.16 mmol) was added to this solution. After 30 min, 30 mL of toluene was added, and the reaction mixture was heated at reflux in a total of 1 h 30 min. After this time more toluene was added, and the reaction was quenched with aqueous HCl. The organic phase was separated and extracted several times with distilled water until the water phase became neutral (pH = 6−7). The organic layer was dried in a Dean−Stark apparatus. The workup was done as described above. Thus 886 mg (71.10%) of yellow polymer was obtained. GPC (THF): $\bar{M}_w$ = 253 200, $\bar{M}_n$ = 60 400, polydispersity index = 4.1. ^{1}H NMR (250 MHz, $CDCl_3$): δ/ppm = 0.77−2.09 (100H, $-CH(CH_2CH_3)(CH_2)_3-$ and $CH_3(CH_2)_{16}-$), 3.98 (8H, $-OCH_2-$), 6.95−7.43 (16H, aromatic and vinylene H's). ^{13}C NMR (62 MHz, $CDCl_3$): δ/ppm = 11.72,(CH_3- ethyl) 14.49 (CH_3- hexyl and octadecyl), 23.07, 23.51, 24.66, 26.47, 29.69, 29.75, 30.05, 30.11, 31.38, 32.31 ($-CH_2-$ ethylhexyl and octadecyl), 40.18 (−CH− ethylhexyl). IR(KBr): 3051 (w, C_{phenyl}−H), 2922 and 2851 (vs, CH_3 and $-CH_2-$), 2202 (vw, disubst −C≡C−), 1636 and 1603 (m, aromatic −C=C−), 1210 (s, C_{aryl}−OR), 964 (m, *trans*-CH=CH−) cm^{-1}. UV−vis ($CHCl_3$): λ_{max}/nm (ϵ/(L. mol^{-1} cm^{-1})) 303.6, 344.0, 449.6 (110 078). Anal. Calcd for $(C_{84}H_{124}O_4)_n$ (1197.90)$_n$: C, 84.22; H, 10.43. Found: C, 81.06; H, 10.86.

Poly[1,4-phenyleneethynylene-1,4-(2,5-di(2-ethylhexyl)oxyphenylene)-1,4-phenyleneethene-1,2-diyl-1,4-(2,5-dioctadecyloxyphenylene)ethene-1,2-diyl] (4da). Dialdehyde **1d** (868 mg, 1.47 mmol) and bisphosphonate **3a** (1.345 mg, 1.47 mmol) were dissolved in dried toluene (60 mL) while stirring vigorously under argon and heating under reflux. Potassium *tert*-butoxide (660 mg, 8 mmol) was added to this solution. After 30 min, 40 mL of toluene was added, and the reaction mixture was heated at reflux in total for 2 h. After this time more toluene was added and the reaction was quenched with aqueous HCl. The workup was done as described above. Thus 1.528 g (86.77%) of yellow polymer was obtained. GPC (THF): $\bar{M}_w$ = 130 100, $\bar{M}_n$ = 42 320, polydispersity index = 3.0. ^{1}H NMR (250 MHz, $CDCl_3$): δ/ppm = 0.77−2.09 (100H, $-CH(CH_2CH_3)(CH_2)_3-$ and $CH_3(CH_2)_{16}-$), 3.85 and 3.99 (8H, $-OCH_2-$), 6.95−7.43 (16H, aromatic and vinylene H's). IR(KBr): 3058 (w, C_{phenyl}−H), 2923 and 2851 (vs, CH_3 and $-CH_2-$), 2203 (vw, disubst −C≡C−), 1598 (w, aromatic −C=C−), 1210 (s, C_{aryl}−OR), 964 (m, *trans*-CH=CH−) cm^{-1}. UV−vis ($CHCl_3$): λ_{max}/nm (ϵ/(M^{-1} cm^{-1})), 344.0 (28 622), 448.0 (98 560), 553.6 (4254). Anal. Calcd for $(C_{84}H_{124}O_4)_n$ (1197.90)$_n$: C, 84.22; H, 10.43. Found: C, 82.68; H, 10.86.

Poly[1,4-(2,5-dioctyloxyphenylene)ethynylene-1,4-(2,5-dioctadecyloxyphenylene)-1,4-(2,5-dioctyloxyphenylene)-ethene-1,2-diyl-1,4-(2,5-dioctyloxyphenylene)ethene-1,2-diyl] (5c). Dialdehyde **2** (923 mg, 0.66 mmol) and bisphosphonate **3c** (424 mg, 0.66 mmol) were dissolved in dried toluene (40 mL) while stirring vigorously under argon and heating under reflux. Potassium *tert*-butoxide (315 mg, 2.80 mmol) was added to this solution; and the reaction mixture was heated at reflux for 1 h 45 min. After this time more toluene was added, and the reaction was quenched with aqueous HCl. The organic phase was separated and extracted several times with distilled water until the water phase became neutral (pH = 6−7). The organic layer was dried in a Dean−Stark apparatus. The resulting toluene solution was filtered, evaporated under vacuum to the minimum, and precipitated in methanol. The polymer was extracted with methanol for 24 h, dissolved once more in toluene, reprecipitated in methanol, and dried under vacuum. Thus 800 mg (71%) of orange red polymer was obtained.

GPC (THF): $\bar{M}_w$ = 82 500, $\bar{M}_n$ = 29 500, polydispersity index = 2.8. VPO ($CHCl_3$): $\bar{M}_n$ = 27 000. ^{1}H NMR (400 MHz, $CDCl_3$): δ/ppm = 0.85−2.01 (60H, m,$CH_3(CH_2)_{16}-$ and CH_3-$(CH_2)_6$), 3.62−4.09 (16H, m, $-CH_2O-$), 6.71−6.83 (2H, m, ^3J = 14.94 Hz, *trans*-CH=CH−)0.00−7.13 (8H, C_{phenyl}−H's), 7.42−7.46 (2H, d, ^3J = 16.90 Hz, *trans*-CH=CH−). ^{13}C NMR (100 MHz, $CDCl_3$): δ/ppm = 14.00, 21.20, 22.62, 25.29, 26.06, 29.44, 31.84, 34.11 ($CH_3(CH_2)_{16}-$ and $CH_3(CH_2)_6$), 69.43, 69.83, 70.02 ($-CH_2O-$), 90.83, 91.99 (−C≡C−), 110.82, 111.18 (C_{aryl}−H ortho to −CH=CH−), 113.11, 114.56 (C_{phenyl}−C≡C−), 117.49 (C_{aryl}−H, ortho to −C≡C−) 123.31, 124.52 (−CH=CH−), 126.90, 127.53, 128.82 (C_{phenyl}−C) 150.60, 151.21, 153.57, 154.12 (C_{phenyl}−OR). IR(KBr): 3057 (w, C_{phenyl}−H), 2924 and 2854 (vs, CH_3 and $-CH_2-$), 2203 (vw, −C≡C−), 1696 (vw, terminal −CHO), 1600 (w, aromatic −C=C−),1206 (s, C_{aryl}−OR), 971 (m, trans −CH=CH−) cm^{-1}. UV−vis ($CHCl_3$): λ_{max}/nm (ϵ/(M^{-1} cm^{-1})) 320.8 (28 000), 472.0 (111 160). Anal. Calcd for $(C_{116}H_{188}O_8)_n$ (1710.76)$_n$: C, 81.44; H, 11.07. Found: C, 81.25; H, 10.89.

Poly[1,4-(2,5-dioctyloxyphenylene)ethynylene-1,4-(2,5-dioctadecyloxyphenylene)-1,4-(2,5-dioctyloxyphenylene)-ethene-1,2-diyl-1,4-(2,5-dioctadecyloxyphenylene)ethene-1,2-diyl] (5a). Dialdehyde **2** (1.038 g, 0.75 mmol) and bisphosphonate **3a** (686 mg, 0.75 mmol) were dissolved in dried toluene (40 mL) while stirring vigorously under argon and

heating under reflux. Potassium *tert*-butoxide (500 mg, 4.45 mmol) was added to this solution; and the reaction mixture was heated at reflux for 2 h. After this time, more toluene was added, and the reaction was quenched with aqueous HCl. The organic phase was separated and extracted several times with distilled water until the water phase became neutral (pH = 6−7). The organic layer was dried in a Dean−Stark apparatus. The resulting toluene solution was filtered and evaporated under vacuum to the minimum, and the polymer was precipitated in methanol. The polymer was extracted for 8 h with methanol, dissolved once more in toluene, reprecipitated in methanol, and dried under vacuum. Thus 1.22 g (81.70%) of orange red polymer was obtained. GPC (THF): $\bar{M}_w = 62\,370$, $\bar{M}_n = 27\,440$, polydispersity index = 2.2. VPO ($CHCl_3$): $\bar{M}_n$ = 23 600. ^{1}H NMR (400 MHz, $CDCl_3$): δ/ppm = 0.85−1.84 (200H, m,$CH_3(CH_2)_{16}$− and $CH_3(CH_2)_6$), 3.98−4.09 (16H, m, $-CH_2O-$), 6.7−7.47 (12H, vinylene and aromatic H's). IR(KBr): 3056 (w, C_{phenyl}−H), 2924 and 2853 (vs, CH_3 and $-CH_2-$), 2202 (vw, −C≡C−), 1605 (w, aromatic −C═C−),1261 and 1207 (s, C_{aryl}−OR), 972 (m, *trans*-CH═CH−) cm^{-1}. UV−vis ($CHCl_3$): λ_{max}/nm (ϵ/(M^{-1} cm^{-1})) 319.2 (28 060), 468.0 (86 300). Anal. Calcd for $(C_{136}H_{228}O_8)_n$ (1991.30)$_n$: C, 82.03; H, 11.54. Found: C, 79.47; H 11.45.

Conclusion

The synthesis of luminophoric dialdehydes **1a**−**d** and **2** was a prerequisite for the synthesis of high-molecular-weight polymers **4** and **5** using the Horner−Wadsworth−Emmons polycondensation reaction. Compounds with various combinations of side chains have been obtained. Solubility of **4** in common organic solvents is possible when long linear alkoxy, like dodecyl and octadecyl, or branched side chains, like 2-ethylhexyl, are grafted onto the polymer backbone. The thermally stable compounds show thermotropic amd lyotropic behavior on polarized optical microscopy. Triple bonds in the PPV backbone confer these compounds with higher electron affinity than in MEH−PPV and higher fluorescence quantum yields. All polymers of type **4** as well as those of type **5** exhibit respectively identical photophysical behavior in chloroform solution. However the properties in solid state (color, thermal behavior, photoconductivity, absorption, emission and fluorescence quantum yield) depend on the *size*, *geometry*, *position*, and *number* of alkoxy side chains grafted on the polymers backbone. **5a** ($R^1 = R^3 = O(CH_2)_7CH_3$, $R^2 = R^4 = O(CH_2)_{17}CH_3$), for example, behaves as if its conjugated backbone was *dissolved* in a hydrocarbon solvent, which explains the highest photoconductivity ($I_{ph} = 1.1 \times 10^{-9}$ A), detected at the lowest threshold of voltage 10 V, and the highest solid state ϕ_{fl} value of 54% obtained among all the polymers.

References and Notes

(1) Hadziioannou, G., van Hutten, P. F., Eds. *Semiconducting polymers: Chemistry, Physics and Engineering*, 1st ed.; Wiley-VCH: Weinheim, Germany, 2000.
(2) Skotheim, T. J., Elsenbaumer, R. L., Reynolds, J. R., Eds. *Handbook of Conducting Polymers*, 2nd ed.; Dekker: New York, 1998.
(3) Martin, R. E.; Diederich, F. *Angew. Chem.* **1999**, *111*, 1440.
(4) Kraft, A.; Grimsdale, A. C.; Holmes, A. B. *Angew. Chem.* **1998**, *110*, 416.
(5) Burroughes, J. H.; Bradley, D. D. C.; Brown, A. R.; Marks, R. N.; MacKays, K.; Friend, R. H.; Burn, P. L.; Holmes, A. B. *Nature* **1990**, *347*, 539.
(6) Greenham, N. C.; Moratti, S. C.; Bradley, D. D. C.; Friend, R. H.; Holmes, A. B. *Nature* **1993**, *365*, 628.
(7) Hörhold, H.-H.; Helbig, M. *Makromol. Chem. Macromol. Symp.* **1987**, *12*, 229.
(8) Staring, E. G. J.; Demandt, R. C. J. E.; Braun, D.; Rikken, G. L. J.; Kessener, Y. A. R. R.; Venhuizen, A. H. J.; van Kippenberg, M. M. F.; Bouwmans, M. *Synth. Met.* **1995**, *71*, 2179.
(9) (a) Moratti, S. C.; Cervini, R.; Holmes, A. B.; Baigent, D. R.; Friend, R. H.; Greenham, N. C.; Grüner, J.; Hamer, P. J. *Synth. Met.* **1995**, *71*, 2117. (b) Pinto, M. R.; Hu, B.; Karasz, F. E.; Akcelrud, L. *Polymer* **2000**, *41*, 2603.
(10) Gurge, R. M.; Sarker, A.; Lahti, P. M.; Hu, B.; Karasz, F. E. *Macromolecules* **1996**, *29*, 4287.
(11) Lux, A.; Holmes, A. B.; Cervini, R.; Davies, J. E.; Moratti, S. C.; Grüner, J.; Cacialli, F.; Friend, R. H. *Synth. Met.* **1997**, *84*, 293.
(12) (a) Marsella, M. J.; Swager, T. M. *Polym. Prepr.* **1992**, *33* (1), 1196. (b) Marsella, M. J.; Fu, D. K.; Swager, T. M. *Adv. Mater.* **1995**, *7*, 145.
(13) Gillissen, S.; Jonforsen, M.; Kesters, E.; Johansson, T.; Theander, M.; Andersson, M. R.; Inganäs, O.; Lutsen, L.; Vanderzande, D. *Macromolecules* **2001**, *34*, 7294.
(14) (a) Bunz, U. H. F. *Chem. Rev.* **2000**, *100*, 1605. (b) Brizius, G.; Pschirer, G. N.; Steffen, W.; Stitzer, K.; zur Loye, H.-C.; Bunz, U. H. F. *J. Am. Chem. Soc.* **2000**, *122*, 12435.
(15) (a) Egbe, D. A. M.; Tillmann, H.; Birckner, E.; Klemm, E. *Macromol. Chem. Phys.* **2001**, *202*, 2712. (b) Egbe, D. A. M.; Roll, C. P.; Klemm. E. *Des. Monomers Polym.*, in press.
(16) (a) Wadsworth, W. S. *Org. React.* **1977**, *25*, 73. (b) Maryanoff, B. E.; Reitz, A. B. *Chem. Rev.* **1989**, *89*, 863. (c) Hörhold, H.-H.; Opfermann, J. *Makromol. Chem.* **1970**, *131*, 105.
(17) Perahia, D.; Traiphol, R.; Bunz, U. H. F. *Macromlecules* **2001**, *34*, 151.
(18) Elias, H.-G. *An Introduction to Polymer Science*; VCH: Weinheim, Germany, 1997; p 124.
(19) Weder, C.; Wrighton, M. S. *Macromolecules* **1996**, *29*, 5157.
(20) Arbuzow, B. A. *Pure Appl. Chem.* **1964**, *9*, 307.
(21) (a) Dieck, H. A.; Heck, F. H. *J. Org. Chem.* **1975**, *93*, 259. (b) Tohda, Y.; Sonogashira, K.; Hagihara, N. *Tetrahedron Lett.* **1975**, *50*, 4467. (c) Yamamoto, T.; Yamamoto, A. *Bull. Chem. Soc. Jpn.* **1984**, *57*, 752. (d) Yamamoto, T. *Bull. Chem. Soc. Jpn.* **1999**, *72*, 621.
(22) Meier, H.; Aust, H. *J. Prakt. Chem.* **1999**, *341*, 466.
(23) (a) Egbe, D. A. M.; Klemm, E. *Macromol. Chem. Phys.* **1998**, *199*, 2683. (b) Grummt, U.-W.; Birckner, E.; Klemm, E.; Egbe, D. A. M.; Heise, B. *J. Phys. Org. Chem.* **2000**, *13*, 112.
(24) Huang, W. Y.; Gao, W.; Kwei, T. K.; Okamoto, Y. *Macromolecules* **2001**, *34*, 1570.
(25) Greiner, A.; Schmidt, H.-W. Aromatic Main Chain Liquid Crystalline Polymers In *Handbook of Liquid Crystals*; Demus, D., Ed.; Wiley-VCH: Weinheim, Germany, and New York, 1998; Vol. 3.
(26) Pfeiffer, S.; Hörhold, H.-H. *Macromol. Chem. Phys.* **1999**, *200*, 1870.
(27) Yamamoto, T. *Bull. Chem. Soc. Jpn.* **1999**, *72*, 621.
(28) Weder, C.; Wrighton, M. S.; Spreiter, R.; Bosshard, C.; Günter, P. *J. Phys. Chem.* **1996**, *100*, 18931.
(29) (a) Berlman, I. B.; *J. Phys. Chem.* **1970**, *74*, 3085. (b) Nijegorodov, N. I.; Downey, W. S. *J. Phys. Chem.* **1994**, *98*, 5639.
(30) (a) Weder, C.; Wrighton, M. S. *Macromolecules* **1996**, *29*, 5157. (b) Peng, Z. *Polymer News* **2000**, *25*, 185.
(31) Crosby, J. N.; Crosby, G. A. *J. Phys. Chem.* **1971**, *75*, 991.

MA012195G